FLUID QUALITY IN A SELF-PRESSURIZED CONTAINER DISCHARGE LINE

By Hugh M. Campbell, Jr.
Propulsion and Vehicle Engineering Laboratory

NASA

George C. Marshall

Space Flight Center,

Huntsville, Alabama

FLUID QUALITY IN A SELF-PRESSURIZED
CONTAINER DISCHARGE LINE

By

Hugh M. Campbell, Jr.

George C. Marshall Space Flight Center
Huntsville, Alabama

ABSTRACT

35995

The thermal condition of cryogenic fluids in the vertical dis-
charge line during draining of saturated liquid from a self-pressurized
container was investigated. At the discharge line inlet the fluid be-
comes two-phase; however, due to the increased static pressure
while flowing downward in the discharge line the vapor subsequently
condenses. The per cent of evaporation and the distance required to
recondense are dependent upon the type of inlet, rate of discharge,
and initial fluid properties. Equations are derived to predict the
fluid quality and static pressure in the discharge line. Predictions
are made for the maximum fluid quality, the distance required for
vapor condensation, and the vapor variation with elevation. Analyti-
cal and experimental results are compared for moderate container
pressures and discharge line flowrates.

NASA - GEORGE C. MARSHALL SPACE FLIGHT CENTER

NASA-GEORGE C. MARSHALL SPACE FLIGHT CENTER

TECHNICAL MEMORANDUM X-53330

FLUID QUALITY IN A SELF-PRESSURIZED
CONTAINER DISCHARGE LINE

By

Hugh M. Campbell, Jr.

APPLIED MECHANICAL RESEARCH BRANCH
PROPULSION DIVISION
PROPULSION AND VEHICLE ENGINEERING LABORATORY

TABLE OF CONTENTS

LIST OF ILLUSTRATIONS

LIST OF ILLUSTRATIONS (Continued)

LIST OF TABLES

DEFINITION OF SYMBOLS

Symbol	Definition
A	Cross Section Area (m^2)
a	Slope of linearized saturated liquid enthalpy curve versus pressure
b	Intercept of linearized saturated liquid enthalpy curve versus pressure
D	Dynamic pressure (N/cm^2)
d	Discharge line diameter (m)
f	Friction factor
g	Gravitation constant (9.81 m/sec^2)
h	Enthalpy (J/G)
Δh	Enthalpy of vaporization (J/G)
L	Length (m)
p	Static pressure (N/cm^2)
Δp	Change in static pressure (N/cm^2)
Q	Volumetric flowrate (cubic meters per minute)
q	Heat transferred to fluid (J/G)
R	Reynolds number
v	Specific volume (m^3/kg)
w	Weight flowrate (kg/sec)
W	External work (J/G)

DEFINITION OF SYMBOLS (Continued)

Symbol	Definition
x	Gravimetric quality (%)
X	Parameter defined by Martinelli[9]
Y	Parameter defined by Martinelli[6]
y	Volumetric quality (%)
z	Elevation (m)
ϕ	Parameter defined by Martinelli[6]
μ	Viscosity (N sec/m^2)
σ	Surface tension (N/cm)
ψ	Velocity (m/sec)

SUBSCRIPTS

c	Container
f	Frictional
g	Vapor phase
ℓ	Liquid phase
m	Arbitrary plane passing through discharge line
n	Arbitrary plane passing through discharge line
t	Inlet throat
tp	Two-Phase
tt	Turbulent liquid-turbulent vapor flow

DEFINITION OF SYMBOLS (Continued)

SUBSCRIPTS

Symbol	Definition
vt	Viscous liquid-turbulent vapor flow
vv	Viscous liquid-viscous vapor flow
z	Elevational

NASA-GEORGE C. MARSHALL SPACE FLIGHT CENTER

TECHNICAL MEMORANDUM X-53330

FLUID QUALITY IN A SELF-PRESSURIZED
CONTAINER DISCHARGE LINE

By

Hugh M. Campbell, Jr.

SUMMARY

The behavior and conditions of the fluid in the vertical discharge line below a closed tank from which a saturated liquid is being drained were investigated. The saturated liquid, upon entering the discharge line, becomes two-phase due to the velocity component of pressure and subsequently condenses due to increasing liquid head as it travels vertically downward in the container discharge line.

Equations were derived from Bernoulli's Equation, the general energy equation, and the equation of state to express the discharge line static pressure and fluid quality as a function of container pressure, discharge line flowrate, elevation, and fluid properties. Solutions to the equations were obtained by a method of finite differences and by an analytical method. Frictional and inlet pressure losses were considered only in the solution obtained from the method of finite differences. Experimental results are presented and compared with the analytical results.

INTRODUCTION

Present day space vehicles require pressurization of propellant tanks to insure adequate net positive suction head at the propellant pump inlet and to maintain vehicle structural integrity. Adequate net positive suction head must be maintained to prevent pump cavitation, for pump cavitation causes erratic propellant flow that can result in

catastrophic failures. Propellant tanks are also pressurized to assist the thin tank walls in maintaining structural integrity. A loss of propellant tank pressure during powered flight could result in complete structural failure.

Generally, cryogenic propellant tanks are filled at atmospheric pressure, and just prior to flight, are pressurized to subcool the liquid. By this process, liquid vaporization is prevented, and more favorable pump inlet conditions are maintained. Container pressure is maintained during draining by the introduction of a pressurant into the container from an external source.

When a superheated vapor below critical pressure coexists in a container with the same fluid in a subcooled state, a saturated liquid layer will form at the vapor-liquid interface, which is in thermal equilibrium with the vapor, and thermal gradient will extend downward into the liquid. Any disturbance of the vapor-liquid interface brings the subcooled liquid into contact with the superheated vapor, causing vapor condensation with an accompanying drop in tank pressure. This phenomenon has been observed in a container that was oscillated to produce sloshing of the liquid and in some propellant piping systems. In the Saturn systems an inert non-condensing pre-pressurant is used to minimize the effects of the contact between superheated vapor and subcooled liquid.

An alternate pressurization scheme consists of filling the cryogenic container, closing off the container, and allowing the heat that is transferred to the cryogen to saturate the cryogen and increase the container pressure to the required amount. The container can then be drained without the addition of pressurant from an external source. Pressurant addition to the ullage space comes from the evaporation of the bulk liquid at the vapor-liquid interface. As the container pressure drops, sensible heat from the bulk liquid supplies the heat for evaporation. Thus, during container draining, as heat is continuously removed from the bulk liquid, the liquid temperature and tank pressure continuously decrease at a slow rate.

Utilization of self-pressurization in discharging cryogenic propellants precludes any pressure drop due to liquid-vapor interface disturbance, because the liquid is saturated and the vapor is only slightly superheated. No pressurant need be relieved, since the highest container pressure obtained would be the pressure required initially.
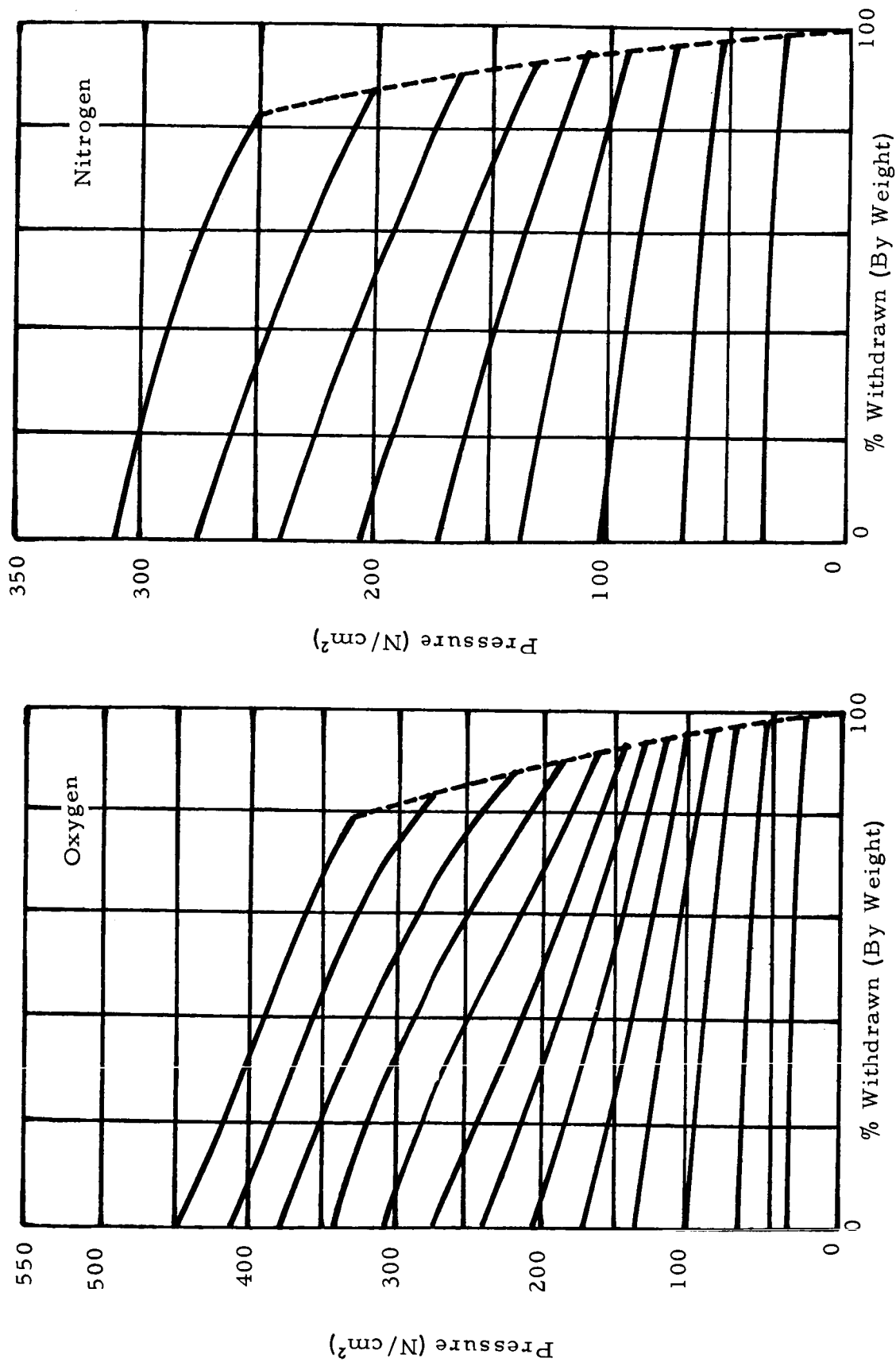
2

FIG 1 Gas Space Pressure versus Liquid Weight Withdrawn for Self Pressurized Cryogen Container

3

The primary disadvantage to the method of self-pressurization is the existance of two-phase fluid flow in the container discharge line. This reduces the mass capacity of a given line size and complicates the accurate control of propellants to the combustion chamber.

In this report the quality of the cryogenic propellant in the vertical discharge line (through which a self-pressurized propellant container is being drained) as a function of container pressure, discharge line flowrate and location, is investigated including the influence of the increased static pressure (liquid head) on a fluid element flowing vertically downward in causing the vapor phase to condense.

RELATED INVESTIGATIONS

In 1960 Canty[1] analyzed the thermodynamics of a cryogenic container, initially full of saturated liquid, when drained adiabatically without the addition of a pressurant. Curves were presented depicting ullage pressure as a function of the initial pressure and the liquid (by weight) removed from the container. A copy of these curves for oxygen and nitrogen are shown in FIG 1. In the energy balance, Canty assumed a saturated liquid leaving the container. Based on this assumption, as the saturated liquid incurs a velocity in leaving the container, the velocity or dynamic pressure will increase at the expense of static pressure, causing two-phase flow in the discharge line. While flowing downward in the discharge line, the fluid static pressure increases due to the elevation difference, thus condensing the vapor phase if frictional pressure losses are not too great.

TWO-PHASE FLUID FLOW

Two-phase fluid flow of a monocomponent fluid is the simultaneous flow of a liquid and vapor in a common pipe or tube. Two-phase fluid flow exhibits interesting patterns and is frequently classified according to pattern and the flow condition of each phase. A survey of the literature on two-phase fluid flow in a horizontal tube by Leonhard and McMordie[2] revealed the following flow patterns.

1. Bubble Flow: Flow characterized by the formation of individual bubbles along the upper surface of the tube. Bubble size increases as the fluid flows through the tube.

4

2. Froth Flow: A foam-like mixture of small bubbles intimately mixed with the liquid. Froth flow approaches a homogeneous fluid.

3. Stratified Flow: The flow of the liquid phase along the bottom of the tube, while the vapor phase occupies the upper portion of the tube. The vapor phase flows at a much higher velocity than the liquid at the bottom. The vapor-liquid interface is a sharp, well defined plane.

4. Wavy Flow: Similar to stratified flow except that waves are formed at the vapor-liquid interface.

5. Plug Flow: Flow characterized by the movement of large plugs of liquid through the tube. Plug flow is the pattern likely to exist in the transition from bubble to stratified flow.

6. Slug Flow: Alternate sections of vapor and liquid flowing through the tube. It occurs as the vapor flow increases during plug flow.

7. Annular Flow: The flow of a continuous liquid layer along the tube wall. The vapor flows along the central core of the tube at a much higher velocity than the liquid.

8. Mist Flow: The flow in which fine liquid drops are suspended by surface tension. There is no significant relative velocity between the liquid and vapor phase.

Gravititational force tends to pull the liquid phase to the bottom of a horizontal tube and allows the vapor phase to flow along the top of the tube, because the liquid is more dense than the vapor. The gravitational force then causes wavy, stratified, plug, slug, and bubble flow. In a vertical tube the gravitational force does not separate the phases but rather causes the buoyant force of the vapor phase to oppose downward flow. This causes froth, slug flow, or bubble flow, in which the bubbles are evenly distributed within a typical tube cross section. A map of two-phase fluid flow pattern regions for a

horizontal tube is shown in FIG 2.

$$\text{0.2486}\ \ v_g\ v_\ell\ w/A$$

Mist

Wave $\qquad$ Annular $\qquad$ Bubble or Froth

Slug

Stratified $\qquad$ Plug

$$\frac{5.6322 \times 10^{-6}\, w_\ell}{\sigma\, \mu_\ell\, v_g\, v_\ell^{\,7/6}\, w_g}$$
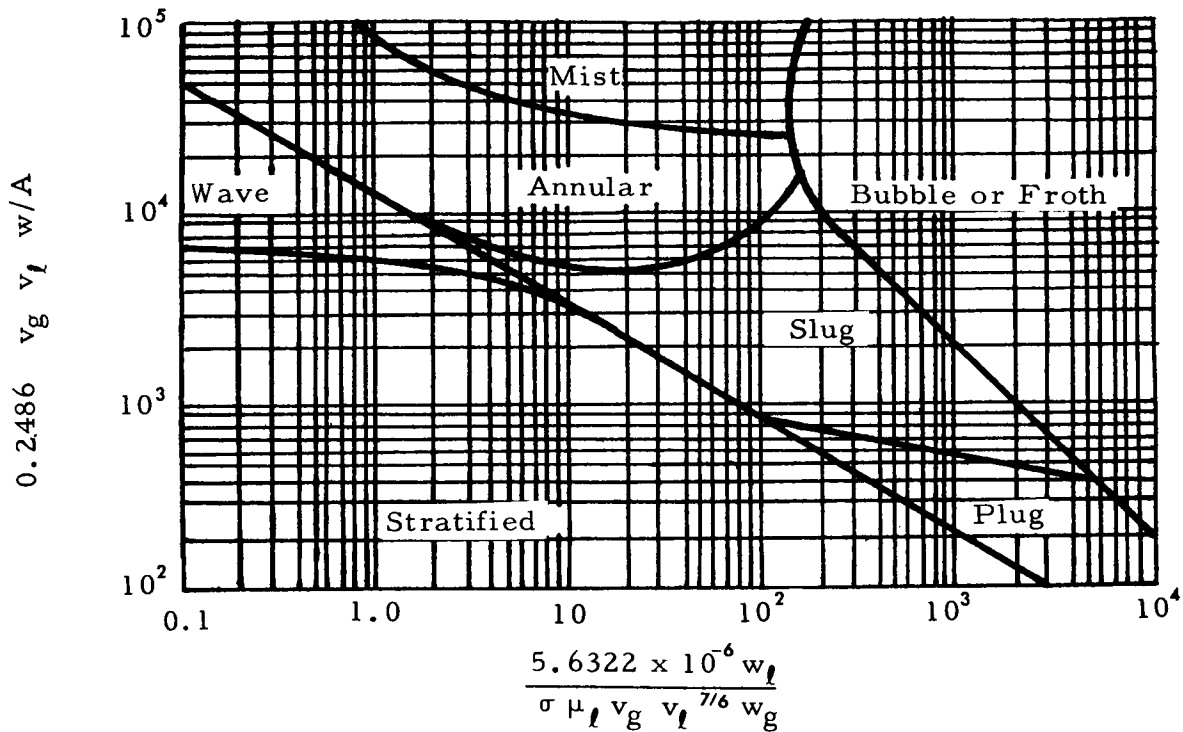
FIG 2 Flow Pattern Regions

Two-phase fluid flow is also classified into the following regimes;

1. Liquid phase turbulent, vapor phase turbulent

2. Liquid phase turbulent, vapor phase viscous

3. Liquid phase viscous, vapor phase turbulent

4. Liquid phase viscous, vapor phase viscous

The criterion for classifying two-phase fluid flow into one of these four regimes is the Reynolds number computed as though the phase in question occupied the complete tube cross sectional area.

TWO-PHASE FRICTIONAL PRESSURE LOSS

Frictional pressure losses in two-phase fluid flow have been studied by many investigators using unique hypotheses and approaches. Some of the earlier and more important contributions are discussed below.

McAdams, Woods and Heroman[3] analyzed the heat transfer coefficient and pressure drop for benzene and lubricating oil flowing inside a heated horizontal tube. They assumed equal velocities for the liquid and vapor phase with a Fanning expression for wall drag and an energy balance to obtain apparent friction factors.

Benjamin and Miller[4] analyzed the pressure drop for flashing water, using the general energy equation and assuming isentropic expansion. The lack of experimental data precludes the use of their analysis for anything other than background literature.

Davidson et al[5] studied heat transmission and frictional pressure drop in boiler tubing using the Fanning frictional pressure loss equation and experimentally determining the friction factor in terms of Reynolds number.

In 1944, Martinelli et al[6] made a major contribution to two-phase fluid flow analysis techniques using the Darcy-Weisbach frictional pressure loss equation and assuming equal static pressure losses for the liquid and vapor phase. A dimensionless parameter ϕg was defined so that:

$$\left(\frac{dp}{dL}\right)_{tp} = \phi_g^2 \left(\frac{dp}{dL}\right)_g \tag{1}$$

or

$$\left(\frac{dp}{dL}\right)_{tp} = \phi_\ell^2 \left(\frac{dp}{dL}\right)_\ell \tag{2}$$

and

$$\phi_g = \phi_g(Y) \tag{3}$$

$$\phi_\ell = \phi_\ell(Y) \tag{4}$$

7

For turbulent liquid, turbulent vapor flow, the parameter Y_{tt} is defined

$$Y_{tt} = \left(\frac{\mu_\ell}{\mu_g}\right)^{0.111} \left(\frac{v_\ell}{v_g}\right)^{0.555} \left(\frac{w_\ell}{w_g}\right) \qquad (5)$$

For viscous liquid, turbulent vapor flow, the parameter Y_{vt} is defined

$$Y_{vt} = (R)^{-0.3} \left(\frac{\mu_\ell}{\mu_g}\right) \left(\frac{v_\ell}{v_g}\right) \left(\frac{w_\ell}{w_g}\right) \qquad (6)$$

ϕ^2_g versus Y_{tt} and Y_{vt} were determined experimentally using air and eight assorted liquids, including benzene, water and SAE-40 oil.

In 1945, Martinelli, Putnam and Lockhart[7] presented data depicting ϕ^2_g in terms of Y_{vv} where Y_{vv} is defined by

$$Y_{vv} = \left(\frac{\mu_\ell}{\mu_g}\right) \left(\frac{v_\ell}{v_g}\right) \left(\frac{w_\ell}{w_g}\right) \qquad (7)$$

ϕ^2_g was determined experimentally in terms of Y_{vv} using air and oil flowing through a capillary tube.

In 1948, Martinelli and Nelson[8] predicted the frictional pressure loss for forced circulation of boiling water using the relationship

$$Y_{tt} = \left(\frac{\mu_\ell}{\mu_g}\right)^{0.143} \left(\frac{v_\ell}{v_g}\right)^{0.571} \left(\frac{1}{x} - 1\right) \qquad (8)$$

with curves for ϕ^2_g and ϕ^2_ℓ versus Y_{tt} from reference 5. The predicted and measured pressure losses agreed within $\pm$ 30 per cent in most cases.

In 1949, Lockhart and Martinelli[9] recorrelated the various parameters related to frictional pressure losses in two-phase fluid flow. In this recorrelation the parameter X_{tt} was defined so that

$$Y_{tt} = X_{tt}^{1.11} \qquad (9)$$

or

$$X_{tt} = \left(\frac{\mu_\ell}{\mu_g}\right)^{0.1} \left(\frac{v_\ell}{v_g}\right)^{0.5} \left(\frac{w_\ell}{w_g}\right)^{0.9} \qquad (10)$$

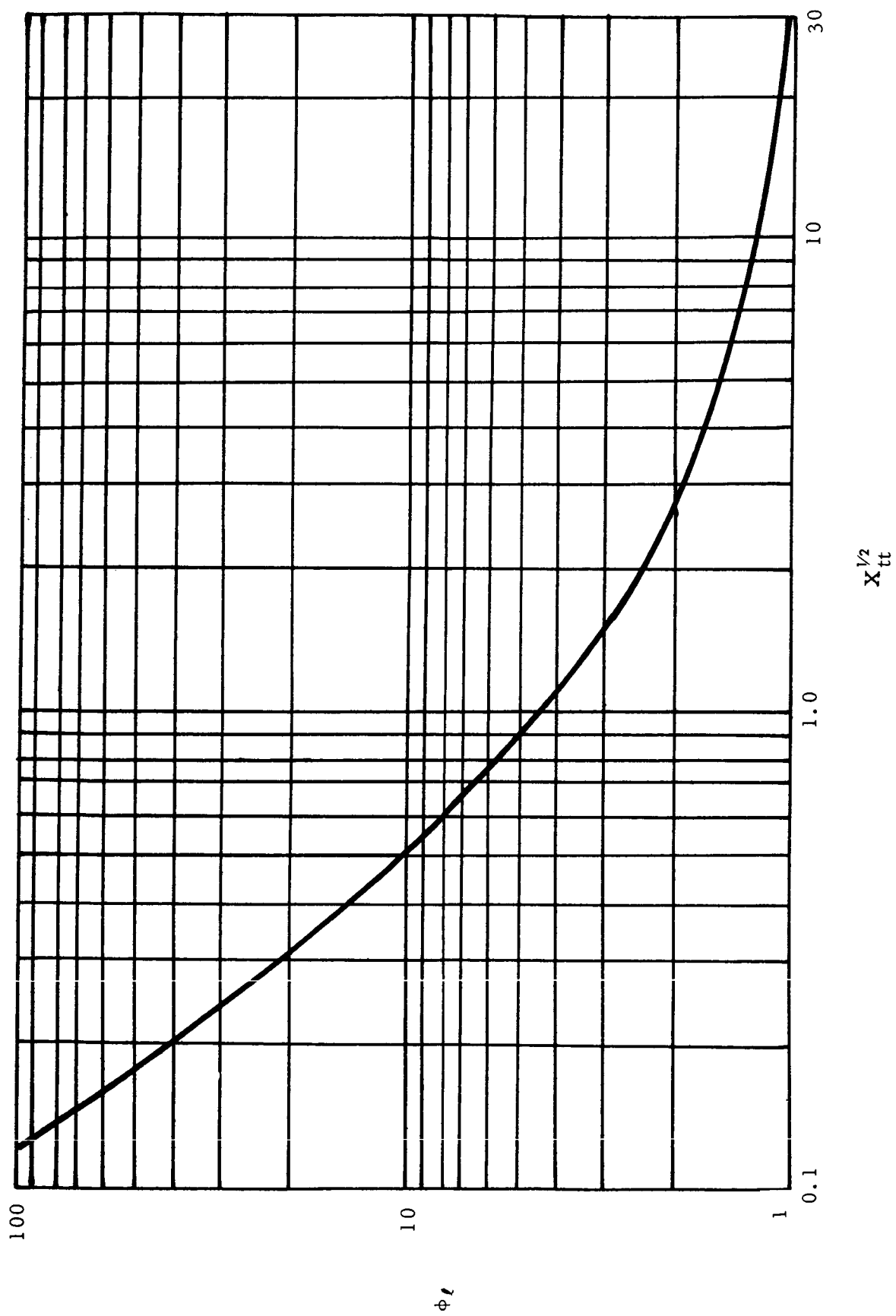ϕ_ℓ is plotted versus X_{tt} in FIG 3.

8

FIG 3 ϕ_ℓ versus $X_{tt}^{1/2}$

Gazely and Bergelen, in a discussion of Lockhart and Martinelli's work, stated that they had obtained data from independent tests using air and water. This data, when analyzed using the parameters of Lockhart and Martinelli, agreed within +20 and -30 per cent of Lockhart and Martinelli's curves.

Throughout Martinelli and associates work a wide spread of data exists, indicating the omission of a pertinent parameter. Gazely and Bergelen postulate that the pertenent parameter could be velocity. Martinelli and associates' data exhibits considerable scatter; however, theirs is the best approximation revealed in the literature. Their analysis is frequently used by other authors for computing two-phase fluid flow frictional pressure loss.

Johnson and Abou-Sabe[10] studied heat transfer and frictional pressure loss for two-phase fluid flow. Their data agreed within +25 and -50 per cent with the data of Martinelli and associates.

Harvey and Foust[11] mathematically derived a relationship for the peak temperature and the vapor head temperature, attained in a long vertical tube evaporator, using the equations of state, energy balance, momentum balance and equation of continuity. The analysis of Martinelli and associates was used to predict frictional pressure loss. Experimental verification proved the analysis, "accurately applicable to experimental data for water below atmospheric pressure".

Rogers[12] analyzed the flow of flashing liquid hydrogen based on the data and analysis of Harvey and Foust, and Lockhart and Martinelli. No experimental data were presented; however, the following equations were derived using the data of Lockhart and Martinelli.

$$\phi_{\ell}^2 = 13.054 X_{tt}^{-1.36} + 2.5996 \qquad \text{for } 0 \le X \le 0.9 \qquad (11)$$

$$\phi_{\ell}^2 = 15.843 X_{tt}^{-0.659} \qquad \text{for } 0.9 \le X \le 26.0 \quad (12)$$

Hatch and Jacobs[13] studied frictional pressure loss in two-phase fluid flow using trichloromonofluoromethane and hydrogen. Their data was 10 to 30 per cent lower than that of Martinelli and associates when ϕ_{ℓ} versus X was plotted. Hatch and Jacobs attribute part of this inconsistency to the probable existence of thermodynamic metastability.

CRYOGEN PROPERTIES

The physical and thermodynamic properties of many of the cryogenic fluids and the properties of many structural materials at cryogenic temperatures have been studied extensively by the National Bureau of Standards, Cryogenic Engineering Laboratories.

Johnson [14] published curves showing density, expansivity, thermal conductivity, specific heat, enthalpy, heat of vaporization, heat of fusion, heat of sublimation, phase equilibria diagrams, dielectric constants, adsorptivity, surface tension and viscosity of most of the cryogenic fluids. The thermal expansion, thermal conductivity, specific heat and enthalpy of many engineering materials were also shown. Viscosity, from this reference, for saturated liquid nitrogen and oxygen is plotted versus pressure in FIG 4.

Stewart, Hust and McCarty [15] tabulated the enthalpy, density and entropy for liquid and gaseous oxygen. The enthalpy versus pressure for saturated liquid oxygen from the reference is plotted in FIG 5, enthalpy of vaporization versus pressure in FIG 6, specific volume for saturated liquid versus pressure in FIG 7, and specific volume for saturated vapor versus pressure is shown in FIG 8.

Strobridge [16] tabulated the enthalpy, internal energy, entropy and specific volume of liquid and gaseous nitrogen. From this reference, enthalpy for saturated liquid nitrogen is plotted versus pressure in FIG 5, enthalpy of vaporization versus pressure in FIG 6, specific volume for saturated liquid versus pressure in FIG 7 and specific volume for saturated nitrogen vapor is shown plotted versus pressure in FIG 8.

ANALYSIS

ANALYTICAL SOLUTION

Fluid Conditions in Pipe Inlet

Consider a self pressurized cryogenic container from which a saturated liquid is being drained through a vertical discharge line. As the fluid flows past the container boundary (see FIG 9) it is assumed to be in the liquid state with negligible dynamic pressure. Additional assumptions are (a) thermodynamic equilibrium, (b) homogeneous fluid

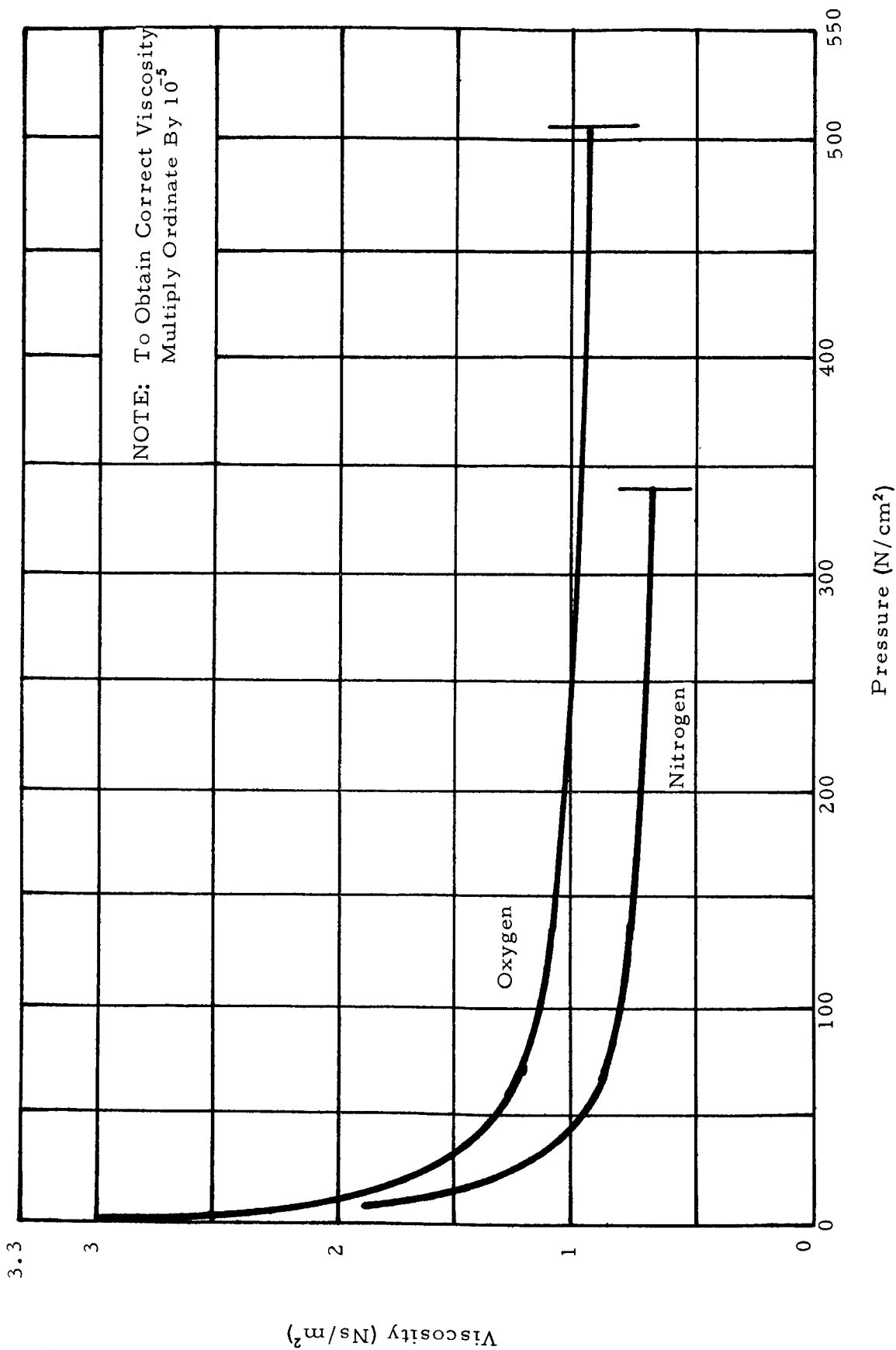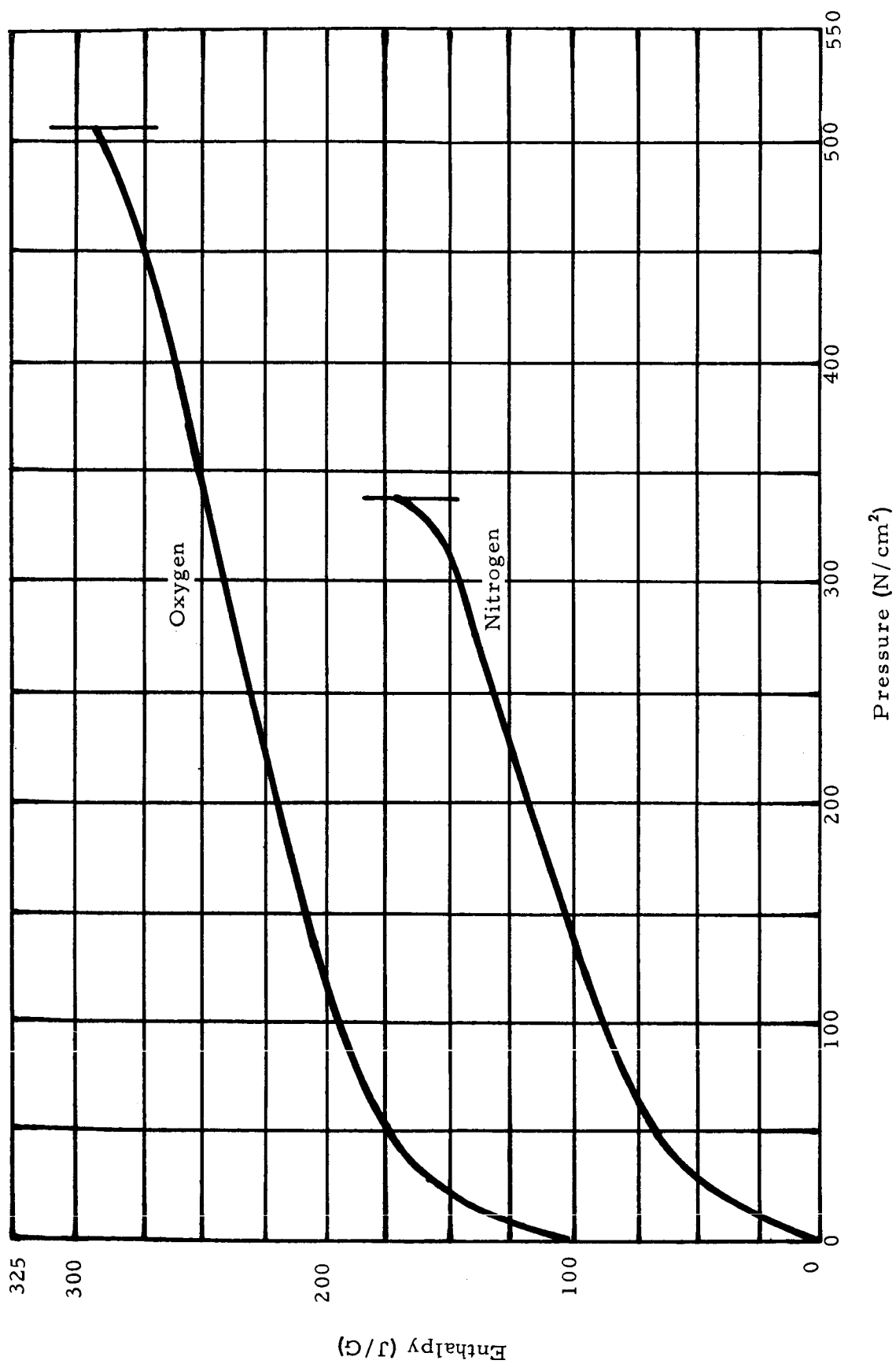FIG 4 Viscosity versus Pressure for Saturated Liquid Nitrogen and Oxygen

12

FIG 5   Enthalpy versus Pressure for Saturated Liquid Nitrogen and Oxygen
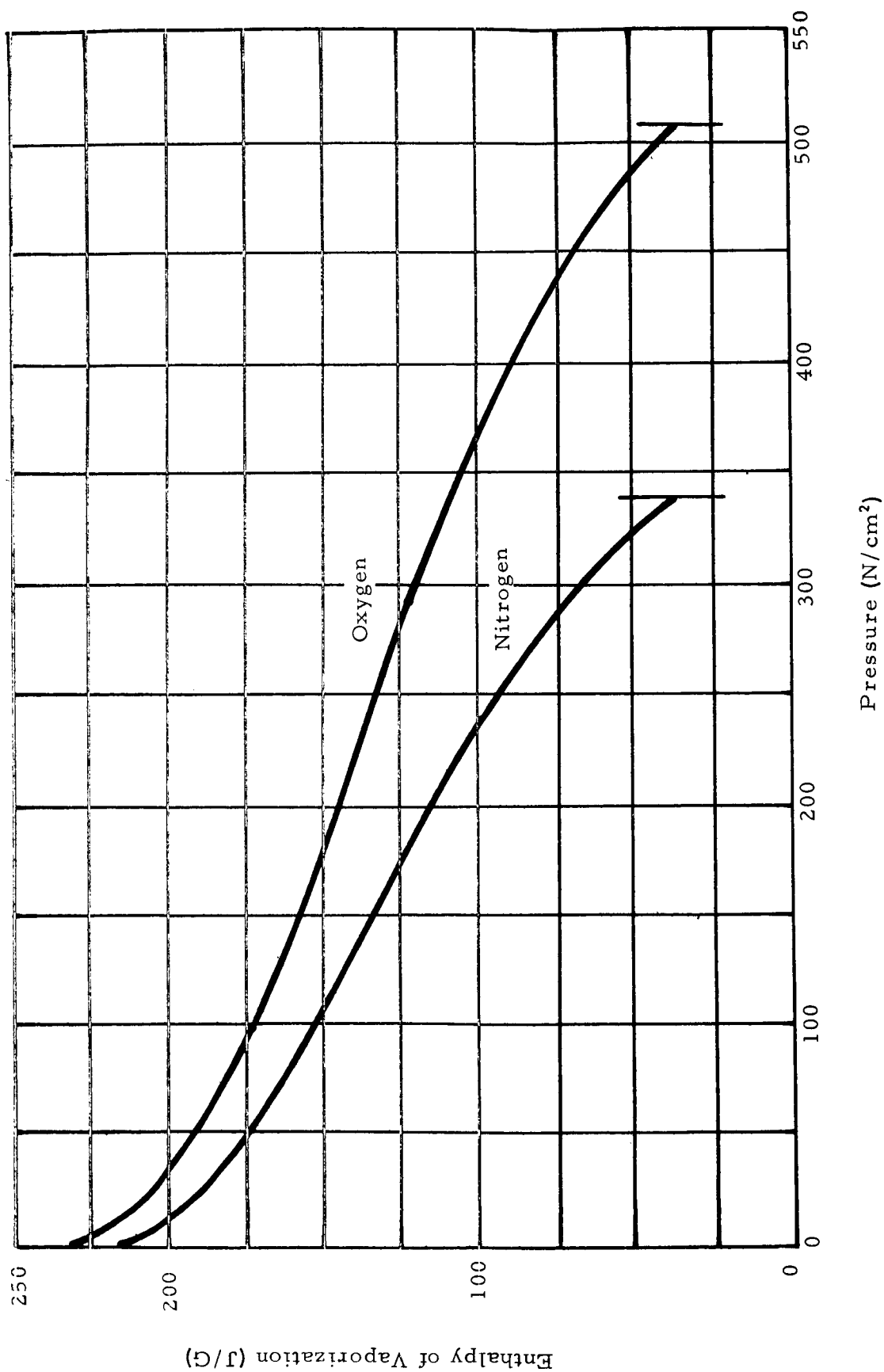
13

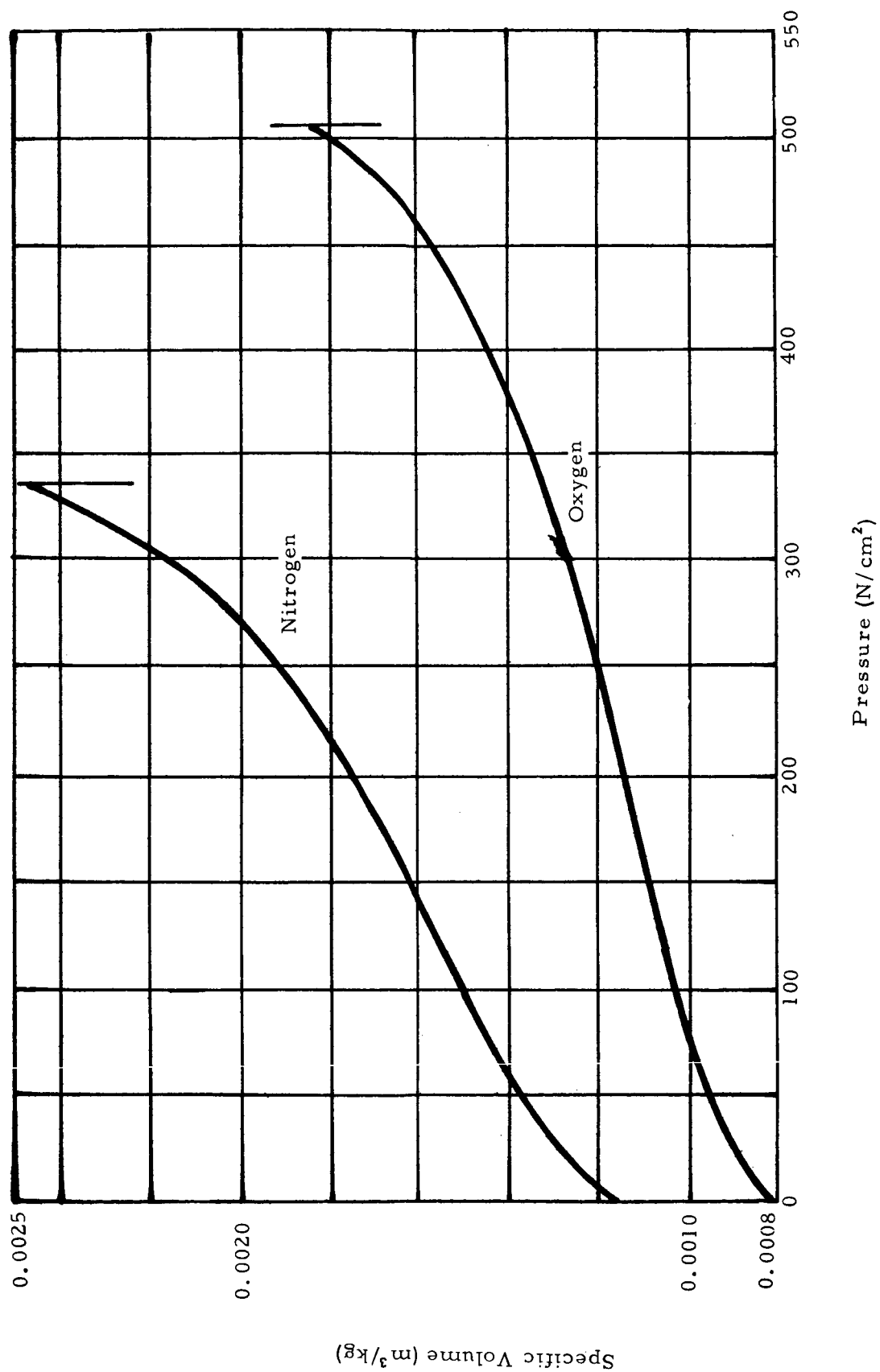FIG 6 Enthalpy of Vaporization versus Pressure for Nitrogen and Oxygen

14

FIG 7 Specific Volume versus Pressure For Saturated Liquid Nitrogen and Oxygen

15
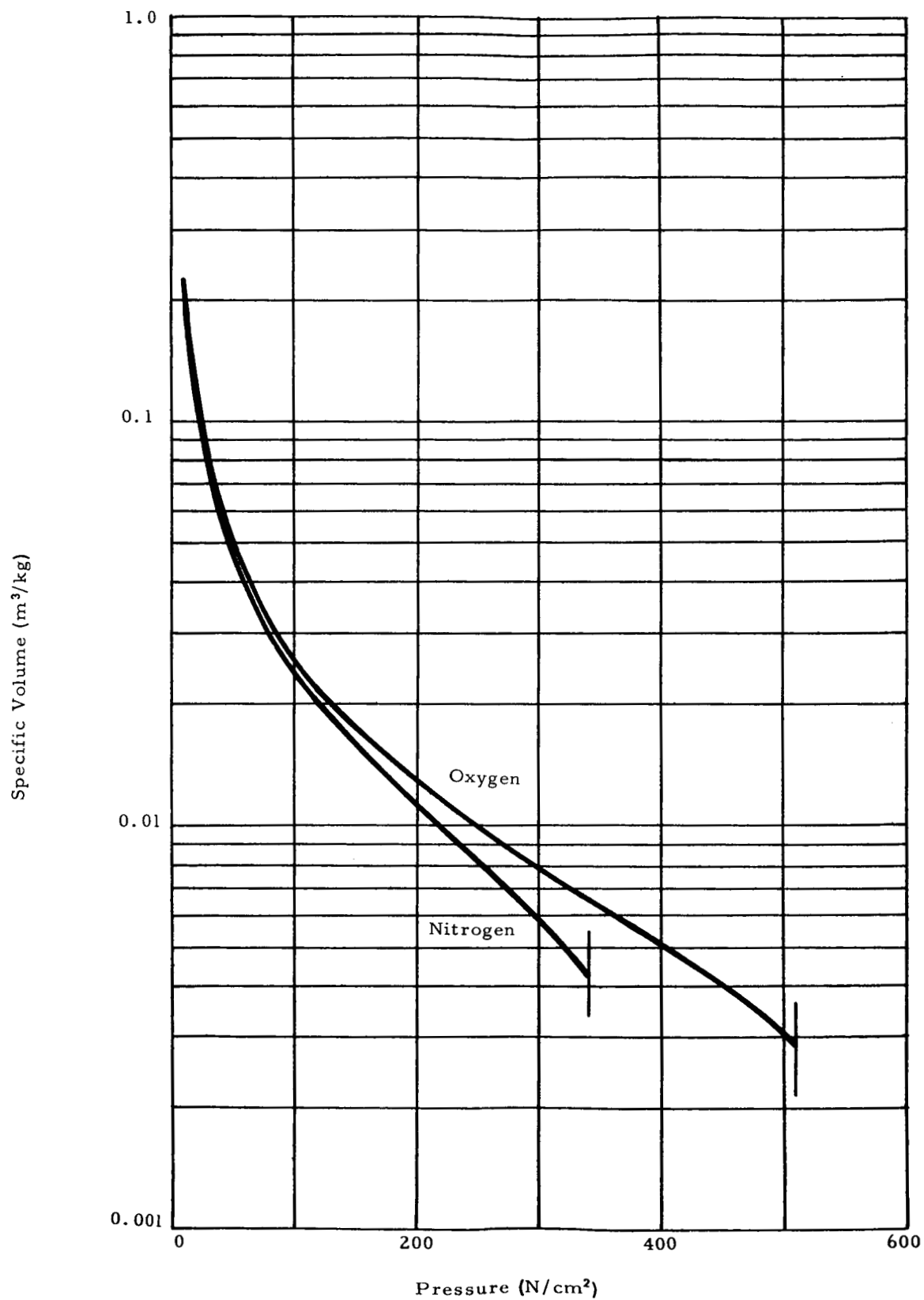
FIG   8   Specific Volume versus Pressure For Saturated Gaseous Nitrogen and Oxygen

16

properties (lumped parameters), (c) no heat transfer to or from the fluid in the inlet, (d) negligible elevation effects and (e) no frictional or inlet pressure losses. The saturated liquid enthalpy is assumed to be a linear pressure function over short pressure ranges, and the
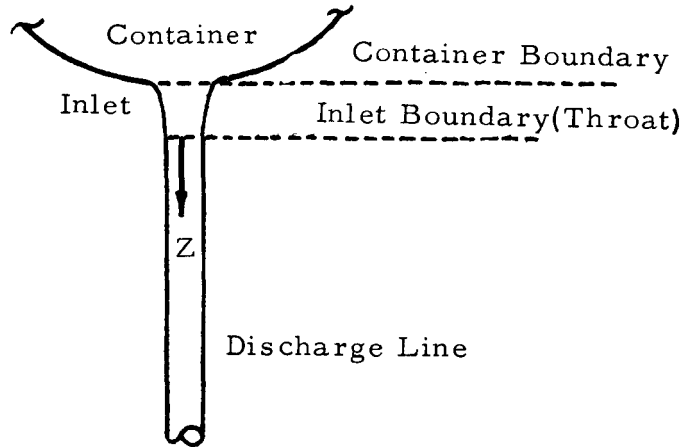
FIG 9 Container, Pipe and Inlet Boundaries

liquid and vapor specific volume and enthalpy of vaporization are assumed to be constant over short pressure ranges. The coordinate system is so chosen that z is positive downward with the origin at the inlet throat.

The differential form of Bernoulli's equation is

$$dp + \frac{10^{-4}\psi d\psi}{v} + \frac{10^{-4} g\, dz}{v} = 0 \tag{13}$$

When elevation effects are excluded, equation 13 becomes

$$dp + \frac{10^{-4}\psi d\psi}{v} = 0 \tag{14}$$

The equation of continuity is

$$\psi = (w/A) \, v \tag{15}$$

In differential form equation 15 becomes

$$d\psi = (w/A)dv + vd(w/A) \tag{16}$$

Substituting equation 15 and 16 into equation 14 and rearranging,

$$10^4 \, dp + \left(\frac{w}{A}\right)^2 dv + v\left(\frac{w}{A}\right)d\left(\frac{w}{A}\right) = 0 \tag{17}$$

Equation 17 is subject to the boundary conditions:

$$p = p_c$$
$$x = 0$$
$$(w/A_c) = 0$$

The specific volume of a two-phase fluid in terms of saturated liquid and vapor specific volume and gravimetric quality is

$$v = (1-x)v_\ell + xv_g \tag{18}$$

In differential form, considering constant liquid and vapor specific volume, equation 18 becomes

$$dv = (v_g - v_\ell) \, dx \tag{19}$$

Substituting equation 18 and 19 into equation 17 gives

$$10^4 dp + (w/A)^2 (v_g - v_\ell)dx + \left[(v_g - v_\ell)x + v_\ell\right](w/A)d(w/A) = 0 \tag{20}$$

In differential form the general energy equation is

$$dh + 10^{-3}\psi d\psi + 10^{-3}gdz + dg - dW = 0 \tag{21}$$

Using the assumptions stated at the first of this chapter, equation 21 becomes

$$dh = 0 \tag{22}$$

The enthalpy of a two-phase mixture in terms of saturated liquid enthalpy, enthalpy of vaporization, and gravimetric quality is given by

$$h = h_\ell + x\Delta h \tag{23}$$

But

$$h_\ell = ap + b \tag{24}$$

So

$$h = ap + b + x\Delta h \tag{25}$$

In differential form equation 25 is

$$dh = adp + \Delta h dx = 0 \tag{26}$$

To determine x_t equation 26 is solved for dp and this value is substituted into equation 20. Equation 20 then becomes, after rearranging,

$$\left[\left(\frac{w}{A}\right)^2 (v_g - v_\ell)\ \frac{10^4 \Delta h}{a}\right]dx + \left[(v_g - v_\ell)\ x + v_\ell\right]\left(\frac{w}{A}\right)d\left(\frac{w}{A}\right) = 0 \tag{27}$$

Solving equation 27 by separation of variables, the result is

$$\left[(v_g - v_\ell)\ x + v_\ell\right]\left[\left(\frac{w}{A}\right)^2 (v_g - v_\ell) - \frac{10^4 \Delta h}{a}\right]^{1/2} = \text{Constant} \tag{28}$$

After incorporation of the boundary conditions, equation 28 becomes

$$x_t = \frac{v_\ell}{v_g - v_\ell}\left[\frac{-\frac{10^4\ \Delta h}{a}}{(w/A)^2 (v_g - v_\ell) - \frac{10^4 \Delta h}{a}}\right]^{1/2} - \frac{v_\ell}{v_g - v_\ell} \tag{29}$$

To determine p_t, equation 26 is integrated subject to the boundary conditions

$$x = 0$$
$$p = p_c$$

The result is

$$p_t = p_c - \frac{x_t \Delta h}{a} \tag{30}$$

Substituting equation 29 into equation 30 gives

$$p_t = p_c + \frac{\Delta h v_\ell}{(v_g - v_\ell)a} - \frac{\Delta h v_\ell}{(v_g - v_\ell)a} \left[\frac{-10^4 \Delta h/a}{(w/A)^2 (v_g - v_\ell) - 10^4 \Delta h/a} \right]^{1/2} \qquad (31)$$

The fluid conditions in the pipe inlet throat are described by equations 29 and 31. These equations will be used with equations developed in the next section to determine the fluid conditions in the cylindrical pipe.

Fluid Conditions in Vertical Pipe Below Inlet

The fluid will cross the exit boundary of the inlet with a quality x_t and pressure p_t determined using equations 29 and 31. Assuming a cylindrical pipe and the same assumptions listed in the previous section, except the velocity effects are neglected and elevation effects are included in Bernoulli's equation, equation 13 becomes:

$$dp + \frac{10^{-4} g \, dz}{v} = 0 \qquad (32)$$

Equation 32 is subject to the boundary conditions

$$z = 0$$
$$x = x_t$$
$$p = p_t$$

The specific volume of a two-phase mixture in terms of saturated liquid and vapor specific volume and gravimetric quality is

$$v = (v_g - v_\ell) x + v_\ell \qquad (33)$$

Substituting equation 33 into equation 32 and rearranging,

$$10^4 \left[(v_g - v_\ell)x + v_\ell \right] dp + g \, dz = 0 \qquad (34)$$

For the case in question, the general energy equation reduces to

$$dh = 0 \qquad (35)$$

20

Using a linearized relationship for the saturated liquid enthalpy over short pressure ranges, substituting this into the relationship for the enthalpy of a two-phase mixture, differentiating, and solving for dp yields:

$$dp = - \frac{\Delta h \, dx}{a} \tag{36}$$

Substituting equation 36 into equation 34 and rearranging

$$\frac{10^4 \, \Delta h}{ga} \left[(v_g - v_\ell) x + v_\ell \right] dx = dz \tag{37}$$

Integrating equation 37 and incorporating the boundary conditions

$$z = \frac{10^4 \, \Delta h}{2ga} \left\{ \left[(v_g - v_\ell) x_t + v_\ell \right]^2 - \left[(v_g - v_\ell) x + v_\ell \right]^2 \right\} \tag{38}$$

To determine the distance required to condense the vapor, set $x = 0$ in equation 38, which yields

$$z = \frac{10^4 \, \Delta h}{2ga} \left\{ \left[(v_g - v_\ell) x_t + v_\ell \right]^2 - v_\ell^2 \right\} \tag{39}$$

Solving equation 38 for x, the quality variation along the discharge line is given by

$$x = \frac{v_\ell}{v_g - v_\ell} \left\{ \left[(v_g - v_\ell) x_t + v_\ell \right]^2 - \left[\frac{(2 \times 10^4) gaz}{\Delta h} \right] \right\}^{0.5} - \frac{v_\ell}{v_g - v_\ell} \tag{40}$$

Integrate equation 36 to determine the variation of quality with pressure; then, using the boundary conditions,

$$p = p_t + \frac{x_t \Delta h}{a} - \frac{\Delta h x}{a} \tag{41}$$

Substituting equation 40 into equation 41

$$p = p_t + \frac{x_t \, \Delta h}{a} - \frac{\Delta h v_\ell}{a(v_g - v_\ell)} \left\{ \left[(v_g - v_\ell) x_t + v_\ell \right]^2 \right.$$
$$\left. - \left[\frac{(2 \times 10^4) gaz}{\Delta h} \right] \right\}^{0.5} + \frac{\Delta h v_\ell}{a(v_g - v_\ell)} \tag{42}$$

21

By using equations 29 and 31 with equations 40 and 42, the fluid conditions can be determined at any discharge line elevation in terms of elevation, container pressure, and weight flowrate per unit cross sectional area.

FINITE DIFFERENCE SOLUTION

Fluid Conditions in Pipe Inlet

Consider a container from which a saturated liquid is being drained through a vertical discharge line. As the fluid flows past the container boundary (FIG 10), it is assumed to be in the liquid state with negligible dynamic head (pressure). Additional assumptions are (a) thermodynamic équilibrium, (b) homogeneous fluid properties and (c) no heat transfer to or from the fluid in the pipe. The coordinate
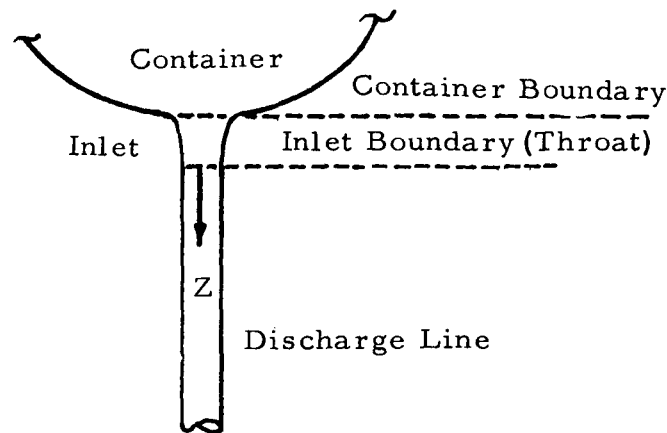
FIG 10 Container, Pipe and Inlet Boundaries

system is so chosen that the positive direction is vertically downward and the origin is at the inlet throat. The pressure of the fluid, as it crosses the container boundary, can be related to the pressure at the inlet throat by

$$p_c + \Delta p_z = p_t + p_t + \Delta p_f \qquad (43)$$

No literature information has been available to predict the frictional and inlet pressure losses between the container and throat, however, in Reference 17, a value of 4 per cent of the dynamic head was recommended for a well shaped bell inlet. From this recommendation, frictional and inlet pressure losses were assumed to be 10 per cent of the dynamic head or,

$$D_t + \Delta p_f = \frac{1.1 \times 10^{-4} \; \psi_t^{\;2}}{v} \tag{44}$$

Combining the equation of continuity and the relationship for specific volume of a two-phase fluid in terms of saturated liquid and vapor specific volume and gravimetric quality gives

$$D_t + \Delta p_f = (1.1 \times 10^{-4}) \; (w/A)^2 \left[(1 - x_t) \, v_{\ell t} + x_t \, v_{gt}\right] \tag{45}$$

The pressure gain due to elevation is given by

$$\Delta p_z = g \times 10^{-4} \int_{z_c}^{z_c} dz/v \tag{46}$$

For small differences in specific volume and elevation, the pressure gain due to elevation can be approximated by:

$$\Delta p_z = \frac{(g \times 10^{-4}) \, [z_t - z_c]}{0.5 \left[v_c + v_t\right]} \tag{47}$$

Substituting the relationship for specific volume of a two-phase mixture in terms of saturated liquid and vapor specific volume and gravimetric quality, noting that the quality crossing the container boundary is zero, gives

$$\Delta p_z = \frac{(2 g \times 10^{-4}) \, [z_t - z_c]}{v_{\ell c} + (1 - x_t) v_{\ell t} + x_t \, v_{gt}} \tag{48}$$

Substituting equations 45 and 48 into equation 43 and rearranging gives

$$p_t = p_c + \frac{(2g \times 10^{-4}) \, [z_t - z_c]}{v_{\ell c} + (1 - x_t) v_{\ell t} + x_t \, v_{gt}} - (1.1 \times 10^{-4}) \; (w/A)^2 \left[(1 - x_t) v_{\ell t} + x_t \, v_{gt}\right] \tag{49}$$

The general energy equation, as applied to the pipe inlet, is

$$h_c + (0.5 \times 10^{-3}) \psi_c^2 + (g \times 10^{-3}) z_c + q = h_t + (0.5 \times 10^{-3}) \psi_t^2 + (g \times 10^{-3}) z_t + W \tag{50}$$

23

Using the assumptions listed, with the relationship for the enthalpy of a two-phase mixture in terms of saturated liquid enthalpy, enthalpy of vaporization and gravimetric quality, and noting that the quality of the fluid crossing the container boundary is zero, equation 50 reduces to

$$h_{\ell c} = h_{\ell t} + x_t \Delta h_t \tag{51}$$

Solving for x_t gives

$$x_t = \frac{h_{\ell c} - h_{\ell t}}{\Delta h_t} \tag{52}$$

Equations 49 and 52 were solved on a digital computer using true fluid properties. Specifying the container pressure and discharge line weight flowrate per unit cross sectional area, and assuming a throat quality x_t, equation 49 is solved for throat pressure. This throat pressure is then used in equation 52 to determine a corrected qualtiy. The corrected throat quality is used in equation 49 to determine a corrected throat pressure. This process is repeated until two consecutive pressures and qualities agree within 0.1 per cent of their absolute value. Throat quality is plotted versus container pressure for several values of w/A for nitrogen in FIG 11 and for oxygen in FIG 12.

Upon examination of equation 52, noting that the enthalpy of a saturated liquid is a function of pressure, it can be seen that the throat quality will be zero, but the fluid will be saturated when the static pressure in the throat and container are equal. Substituting these conditions into equation 49, and noting that since the throat and container pressures are equal, their specific volumes will be equal, and the following relationship is obtained.

$$w/A = \frac{[8.918 \ (z_t - z_c)]^{0.5}}{v_{\ell c}} \tag{53}$$

In the experimental facility used to verify this analysis, the term $z_t - z_c$ was 0.254 meters. Using the value in equation 53, the maximum value of w/A, for which the fluid will remain single phase, is plotted versus container pressure in FIG 13. Any value of w/A greater than the plotted value will result in two-phase flow, and any value below the plotted value will cause subcooled fluid in the pipe inlet throat.
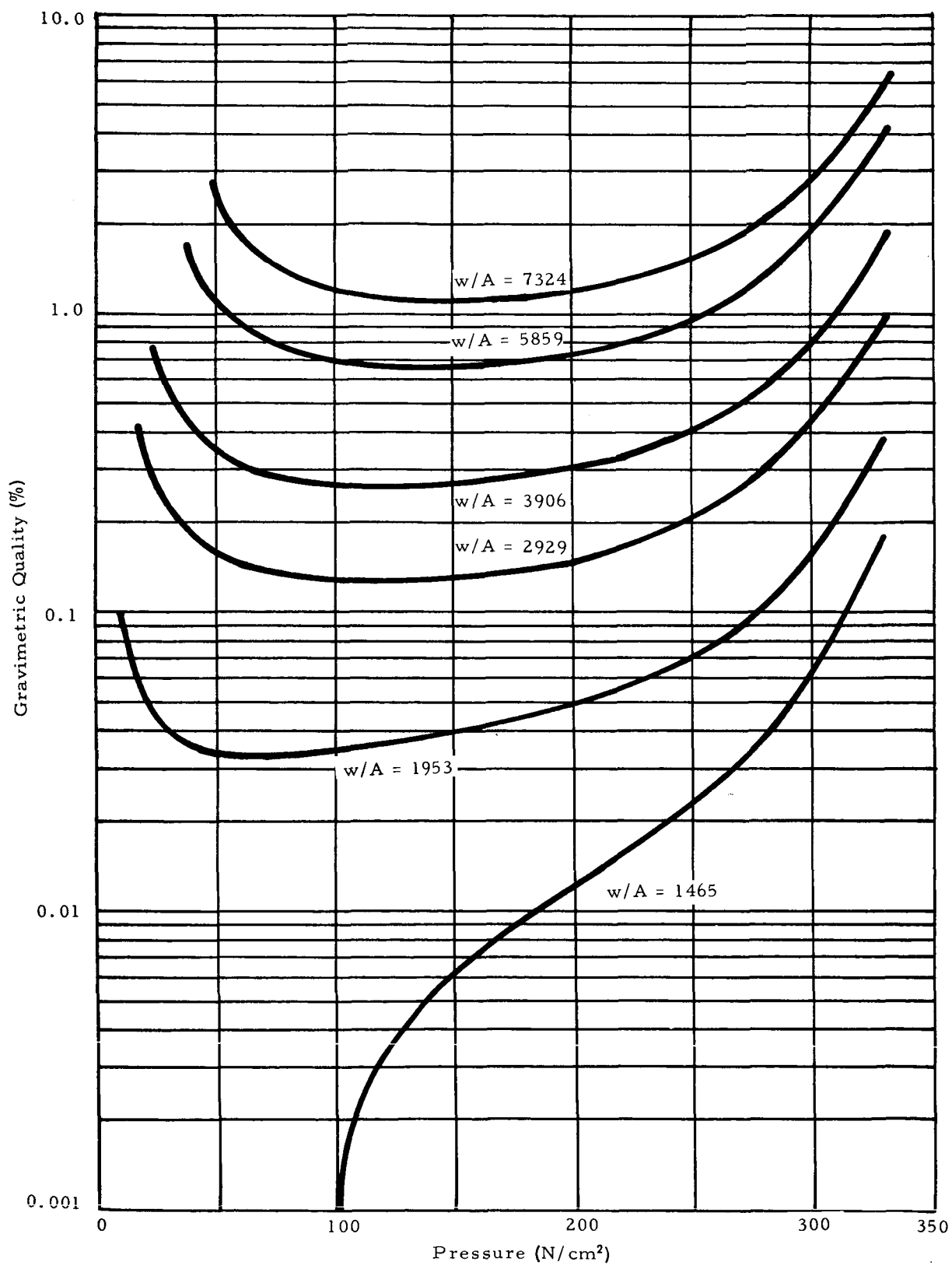
24

FIG 11 Nitrogen Inlet Quality versus Container Pressure (Finite Difference Solution)
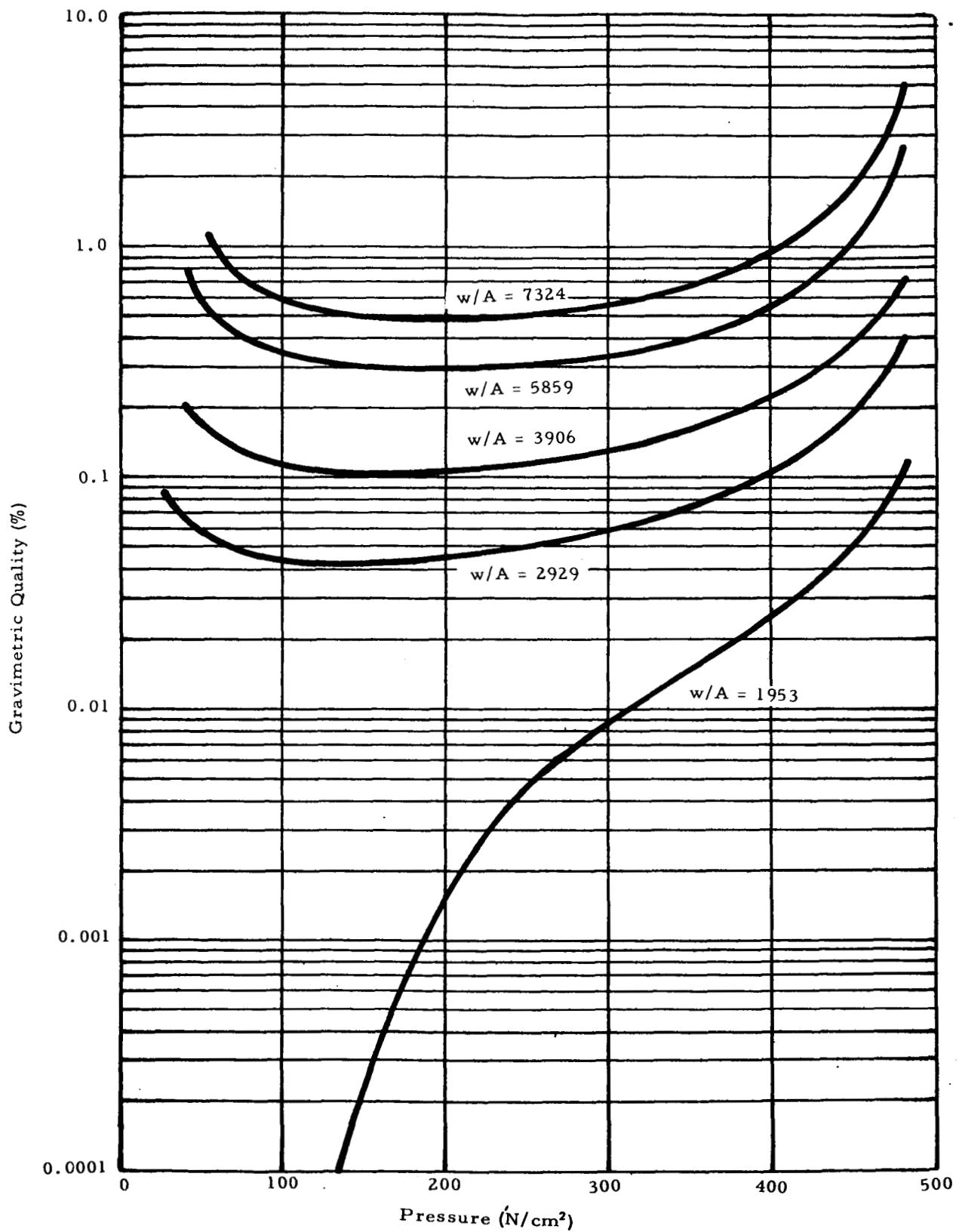
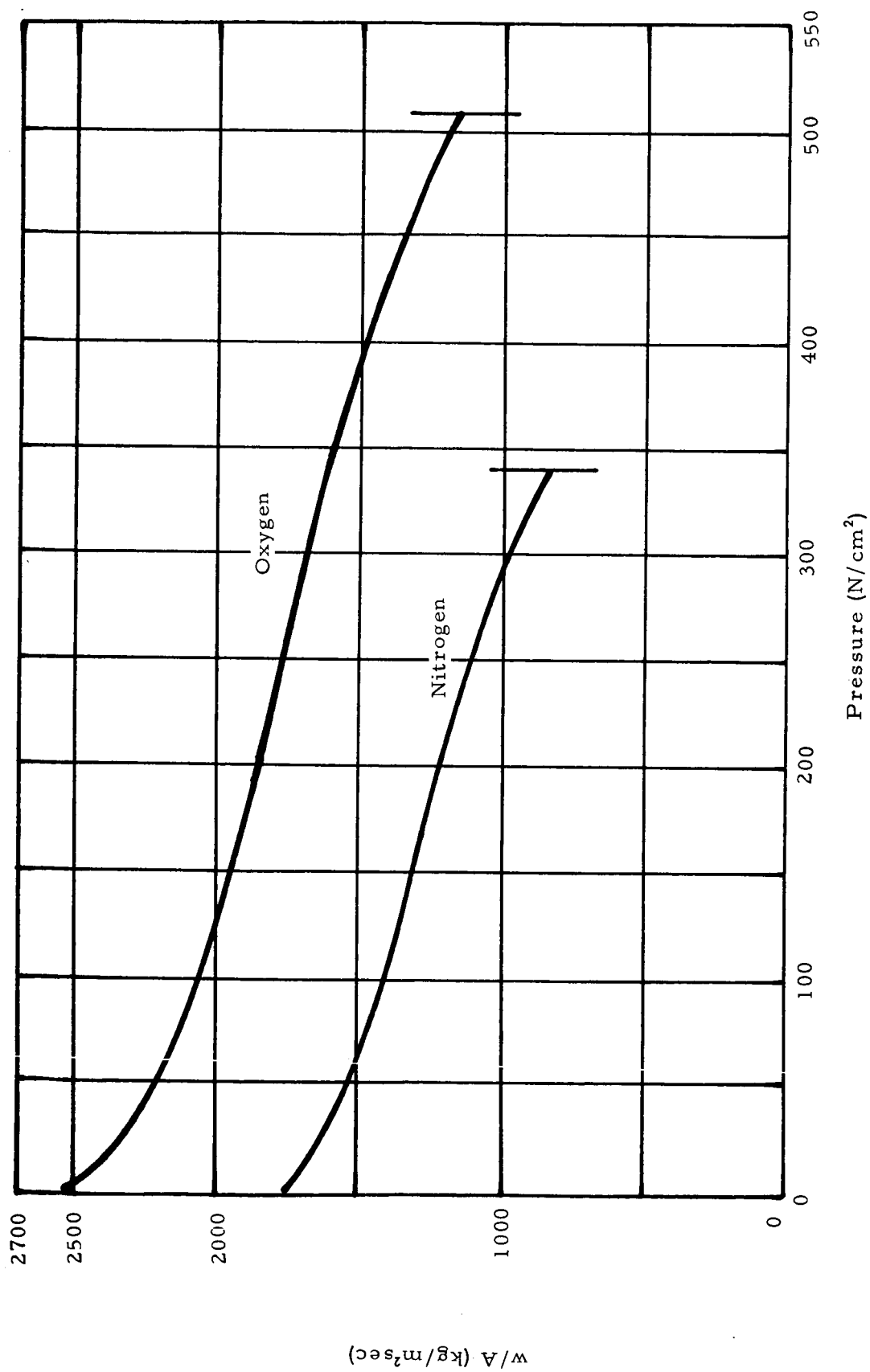FIG   12   Oxygen Inlet Quality versus Container Pressure (Finite Difference Solution)

FIG 13 Maximum Single Phase w/A in Pipe Inlet versus Container Pressure For Nitrogen and Oxygen

27

Fluid Conditions in Cylindrical Pipe Below Inlet

The fluid crosses the exit boundary of the inlet with a quality and pressure that can be determined by using equations 49 and 52. The coordinate system is so chosen that the positive direction is vertically downward and the origin is the inlet throat. Using the same assumptions as in the previous section, the fluid pressure at the arbitrary elevations, z_m and z_n, where $z_m > z_n$ can be related by

$$p_m + D_m + \Delta p_f = p_n + D_n + \Delta p_z \tag{54}$$

where

$$D = \frac{10^{-4} \psi^2}{v} \tag{55}$$

Using the equation of continuity and the relationship

$$v = (1 - x)v_\ell + xv_g \tag{56}$$

equation 55 becomes

$$\left.\begin{aligned}
D_m &= 10^{-4} (w/A)^2 \left[(1 - x_m)\, v_{\ell m} + x_m\, v_{gm}\right] \\[2mm]
D_n &= 10^{-4} (w/A)^2 \left[(1 - x_n)\, v_{\ell n} + x_n\, v_{gn}\right]
\end{aligned}\right\} \tag{57}$$

The pressure gain due to elevation is

$$\Delta p_z = 10^{-4} g \int_{z_n}^{z_m} dz/v \tag{58}$$

For small elevations and specific volume changes, the pressure gain due to elevation can be approximated by

$$\Delta p_z = \frac{2g \times 10^{-4} (z_m - z_n)}{v_m + v_n} \tag{59}$$

Substituting equation 56 into equation 59

$$\Delta p_z = \frac{2g (z_m - z_n) 10^{-4}}{\left[(1 - x_m)v_{\ell m} + x_m\, v_{gm} + (1 - x_n)v_{\ell n} + x_n\, v_{gn}\right]} \tag{60}$$

28

To determine the frictional pressure loss, the analysis of Martinelli and associates[6,7,8,9] is used. All discharge line flow is assumed to be turbulent liquid, turbulent vapor, and only the equations for this case are selected. From reference 6 the relationship for single phase and two-phase frictional pressure loss is

$$\frac{dp}{dz}\bigg|_{tp} = \frac{dp}{dz}\bigg|_{\ell} \phi_{\ell}^2 \tag{61}$$

ϕ_{ℓ}^2 is determined from the following equations:

$$\phi_{\ell}^2 = 13.054 \, X^{-1.36} + 2.5996 \quad \text{for} \quad 0 \le X \le 0.9$$

$$\phi_{\ell}^2 = 15.843 \, X^{-0.659} \quad \text{for} \quad 0 \le X \le 26.0$$

$$\phi_{\ell}^2 = 4.957 \, X^{-0.303} \quad \text{for} \quad 26.0 \le X \le 196.0$$

$$\phi_{\ell}^2 = 1 \quad \text{for} \quad X \ge 196.0$$

$$\tag{62}$$

where

$$X = \left(\frac{v_\ell}{v_g}\right)^{0.5} \left(\frac{\mu_\ell}{\mu_g}\right)^{0.1} \left(\frac{1}{x} - 1\right)^{0.9} \tag{63}$$

Since v_ℓ, v_g, μ_ℓ and μ_g are functions of pressure for a saturated fluid, the function $(v_\ell/v_g)^{0.5}(\mu_\ell/\mu_g)^{0.1}$ is also a function of pressure, and is plotted versus pressure in FIG 14.

The Darcy-Weisbach relationship for frictional pressure loss is

$$\frac{dp}{dz}\bigg|_{\ell} = \frac{4f \, \psi^2 (10^{-4})}{v_\ell \, d} \tag{64}$$

The Blasius relationship for the friction factor for turbulent flow is

$$f = \frac{0.046}{R^{0.25}} \tag{65}$$

$$R = \frac{wd}{A\mu_\ell} \tag{66}$$

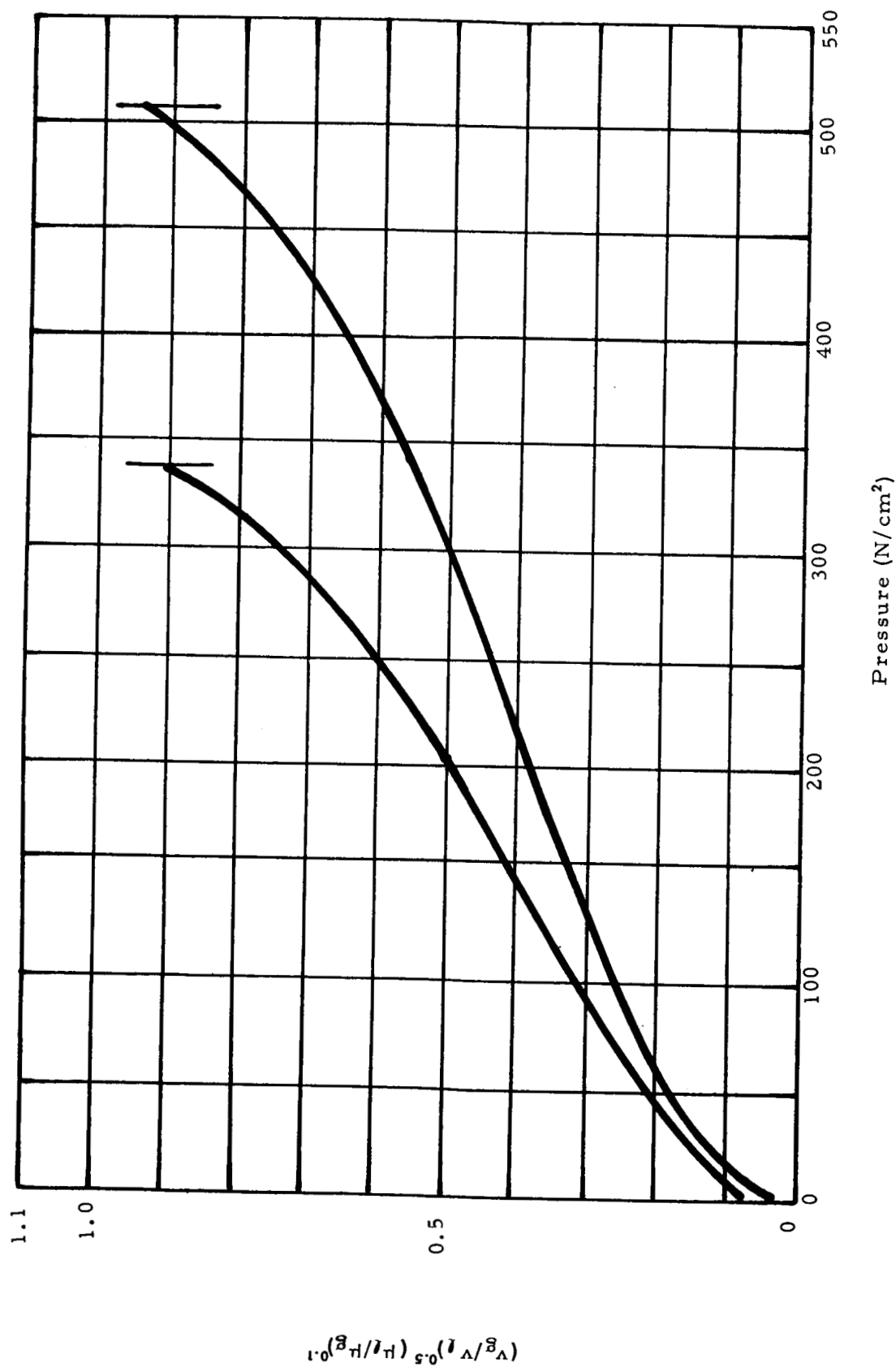Substituting the equation of continuity, equation 65 and 66 into equation

FIG 14 Martinelli's Parameter $(v_g/v_\ell)^{0.5} (\mu_\ell/\mu_g)^{0.1}$ versus Pressure For Nitrogen and Oxygen

Pressure (N/cm^2)

$(v_g/v_\ell)^{0.5} (\mu_g/\mu_\ell)^{0.1}$

30

64, then sutstituting this into equation 61 gives

$$\frac{dp}{dz}\bigg|_{tp} = \frac{0.184 \ (w/A)^2 v_\ell \ (10^{-4}) \ \phi_\ell^2}{(wd/A\mu_\ell)^{0.25} \ d}$$ (67)

The frictional pressure loss between elevations z_n and z_m is

$$\Delta p_f = \int_{z_n}^{z_m} \frac{dp}{dz}\bigg|_{tp} dz$$ (68)

For small changes in frictional pressure loss and elevation, the frictional pressure loss can be approximated by

$$\Delta p_f = 0.5 \ (z_m - z_n) \left[\frac{dp}{dz}\bigg|_{tpm} + \frac{dp}{dz}\bigg|_{tpn}\right]$$ (69)

Substituting equation 67 into equation 69 and rearranging,

$$\Delta p_f = \frac{9.2(10^{-6}) \ (z_m - z_n) \ (v_{\ell m}\phi_{\ell m}^2 + v_{\ell n}\phi_{\ell n}^2) \ (w/A)^2}{(wd/A\mu_\ell)^{0.25} \ d}$$ (70)

Substituting equations 57, 60, and 70 into equation 54 and rearranging,

$$P_m = P_n + (w/A)^2 \left[(1-x_m)v_{\ell n} + x_n v_{gn} - (1 - x_m)v_{\ell m} - x_m v_{gm}\right]$$

$$+ \frac{2g(z_m - z_n) \ (10^{-4})}{\left[(1 - x_m)v_{\ell m} + x_m v_{gm} + (1 - x_n)v_{\ell n} + x_n v_{gn}\right]}$$ (71)

$$- \frac{9.2(10^{-6}) \ (w/A)^2 (z_m - z_n) \ (v_{\ell m}\phi_{\ell m}^2 + v_{\ell n}\phi_{\ell n}^2)}{(wd/A\mu_\ell)^{0.25} \ d}$$

The general energy equation relating the energy flowing past the container boundary to the energy flowing past the elevation plane z_m, after incorporation of the assumptions listed earlier, is

$$h_c = h_m$$ (72)

Substituting equation 51 into equation 72 and solving for x_m gives

$$x_m = \frac{h_{\ell c} - h_{\ell m}}{\Delta h_m}$$ (73)

31

Using solutions obtained by equations 49 and 52 as a starting point, the fluid conditions were computed at discrete discharge line elevations in the same manner that equations 49 and 52 were solved. For all combinations computed of container pressure and discharge line flowrate per unit of cross sectional area, the quality was shown to decrease as the fluid moved down the discharge line. The distance required to condense the vapor is plotted versus container pressure for several values of (w/A) for nitrogen in FIG 15 and for oxygen in FIG 16. The variation of quality with elevation is shown for two container pressures and several values of (w/A) for Nitrogen in FIG 17 and for oxygen in FIG 18.

EXPERIMENTAL APPARATUS AND PROCEDURE

EXPERIMENTAL APPARATUS

General Description

The experimental apparatus consisted of a 1.702 meter (68 inches) inside diameter, spherical aluminum tank atop a 12.2 meter (40 foot) tower. A 0.1524 meter (6 inches) inside diameter discharge line and a 0.1015 meter (4 inches) inside diameter recirculation line were suspended vertically underneath the tank and connected near the bottom of the discharge line. The discharge line and inlet were insulated with polyurethane foam to minimize heat transfer. The recirculation line was not insulated, but heat was allowed to flow into the fluid so that a density differential would exist between the fluid inside the recirculation line and the fluid inside the discharge line to promote convective circulation and prevent "geysering". The experimental apparatus is depicted schematically in FIG 19, and a picture of the apparatus is shown in FIG 20. A recirculation valve was used to prevent flow in the recirculation line during draining of the tank. A vent valve was provided atop the tank to relieve tank pressure, and a valve at the bottom of the discharge line was used to drain the container. Discharge line flow was controlled with orifices located immediately upstream of the drain valve. A description of the components used in this apparatus is shown in Table I.

Pressure was measured at two locations in the container, and temperature was measured at five locations. Liquid depth was determined by measuring the difference in static pressure at the top
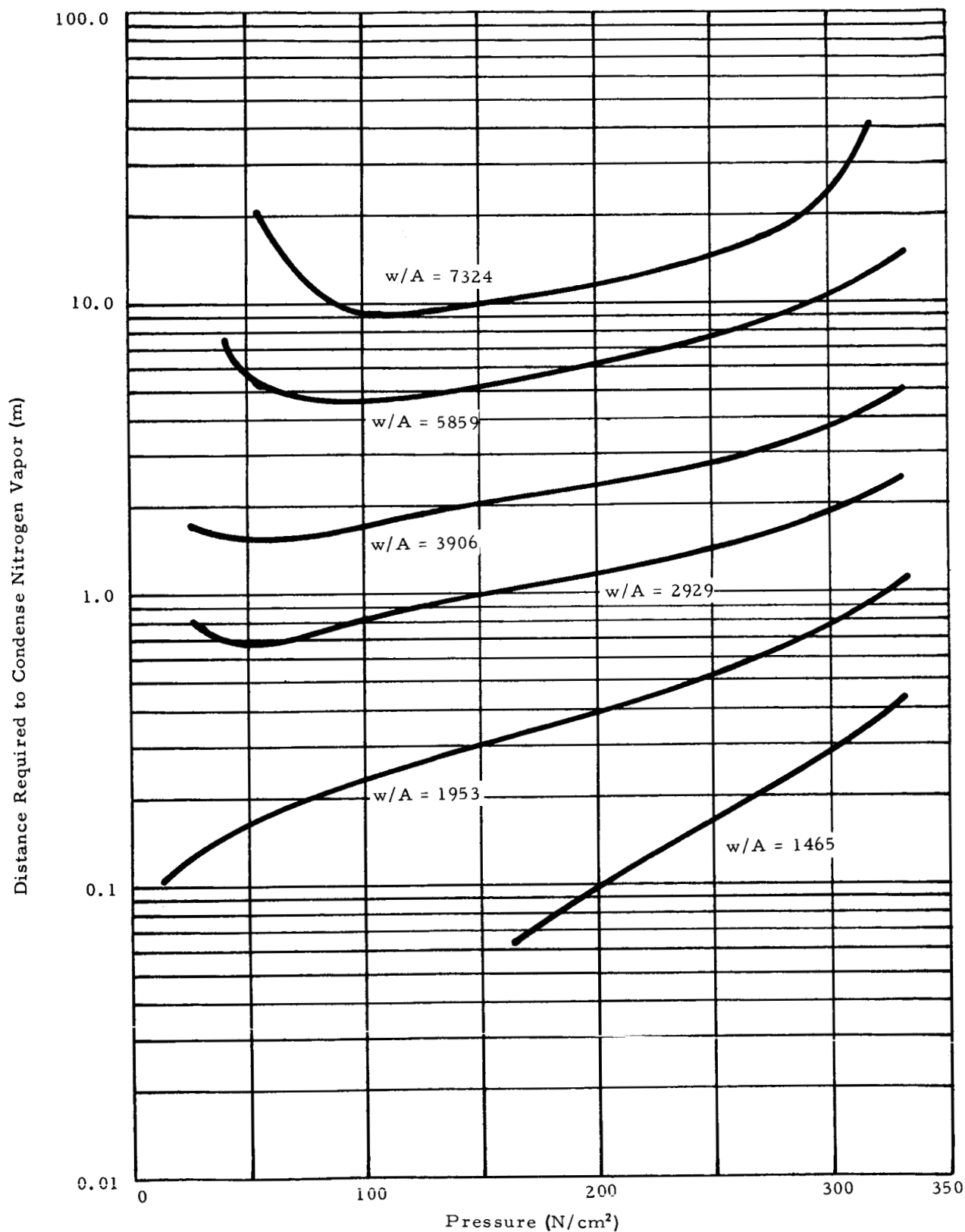
FIG   15   Distance Required to Condense Nitrogen Vapor versus Container Pressure
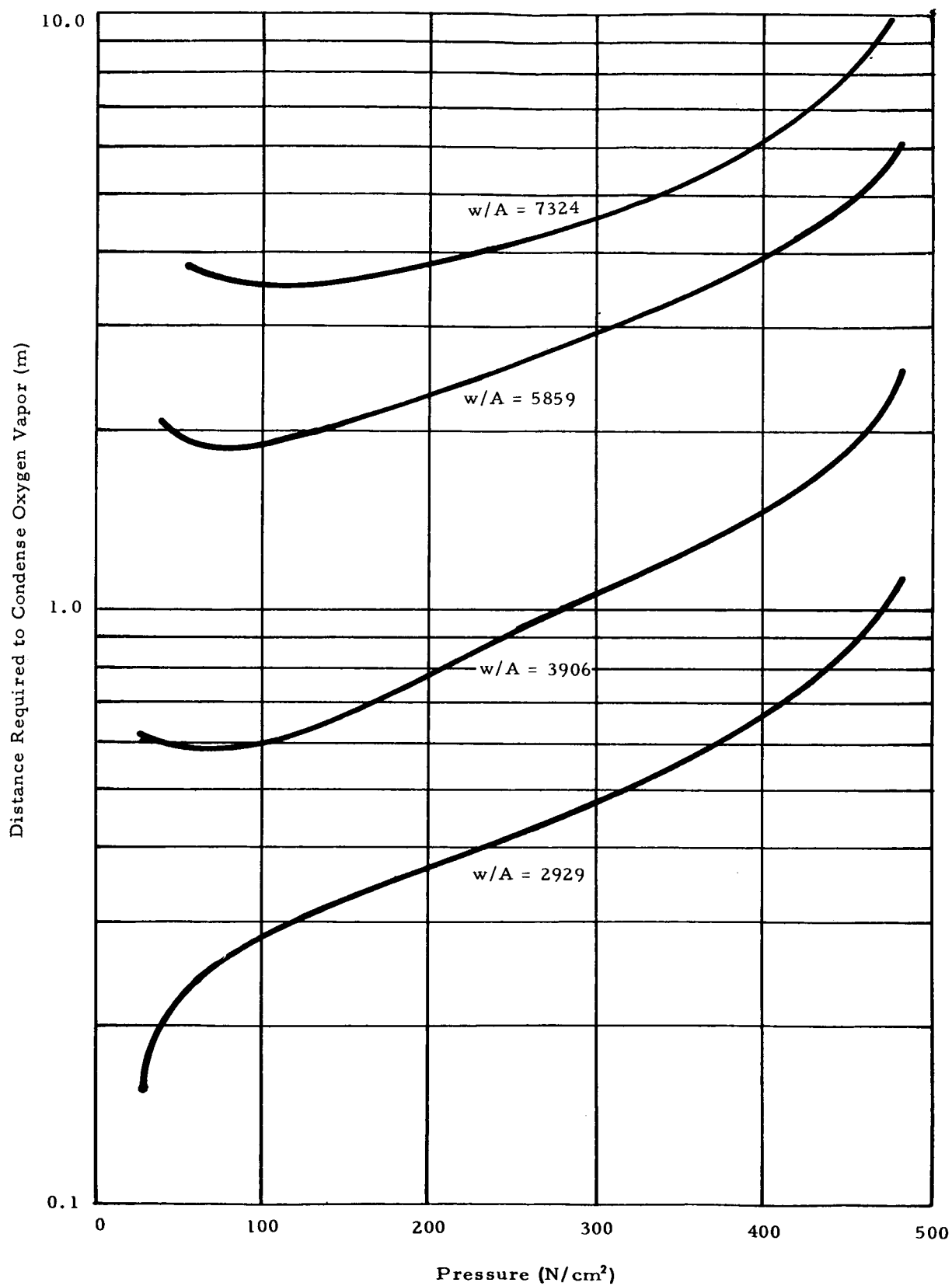(Finite Difference Solution)

FIG 16 Distance Required to Condense Oxygen Vapor versus Container Pressure
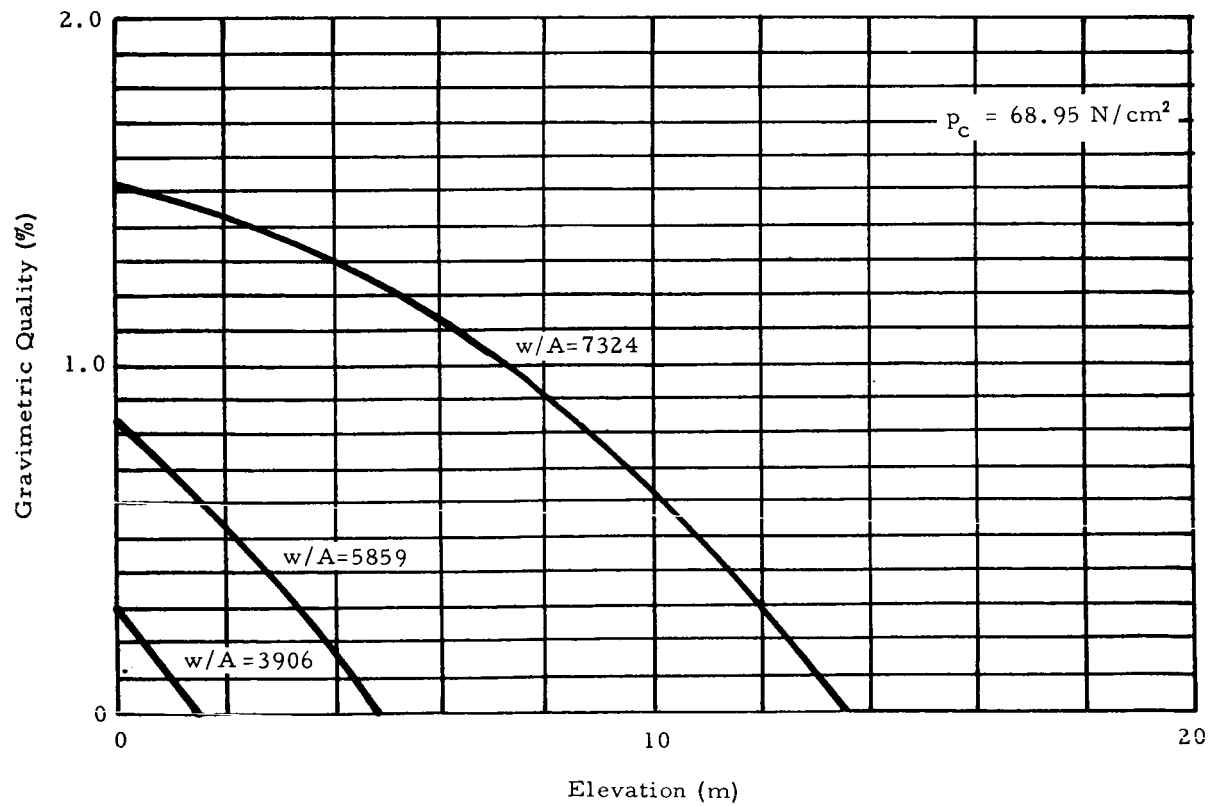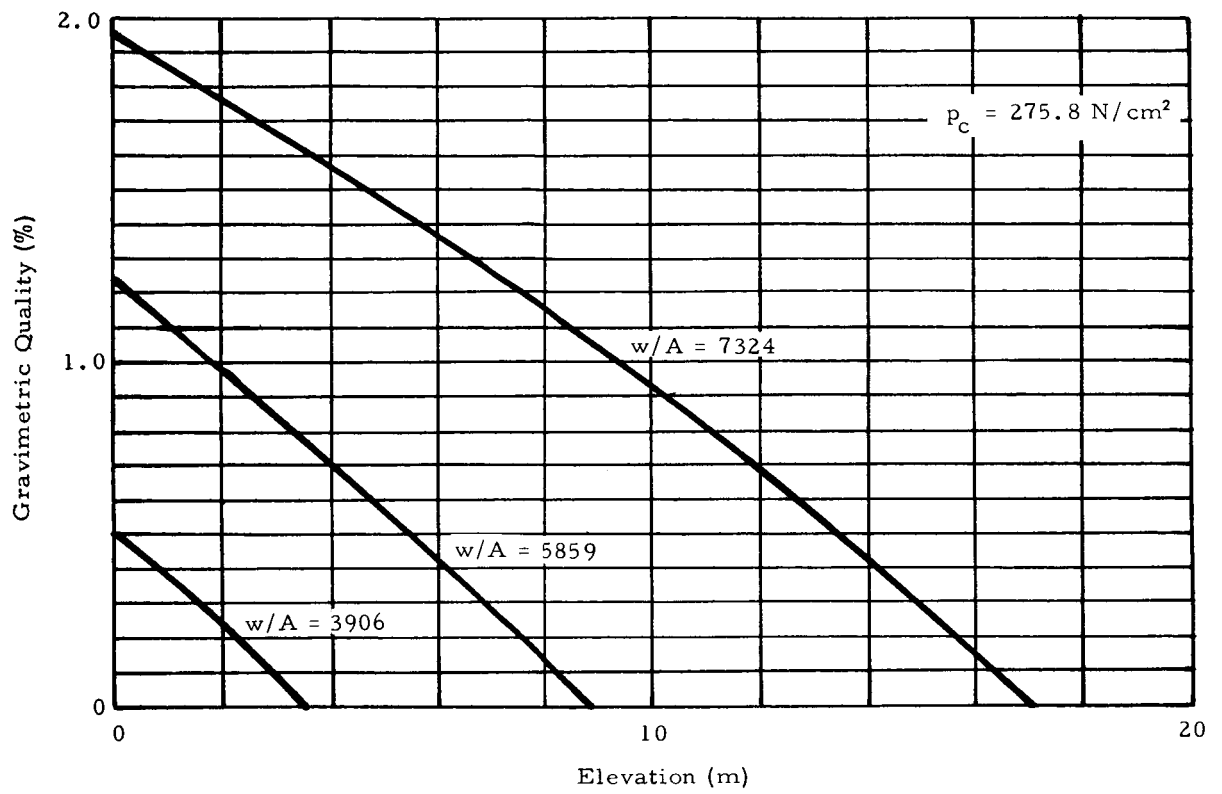(Finite Difference Solution)

34

FIG 17 Quality versus Elevation for Nitrogen (Finite Difference Solution)
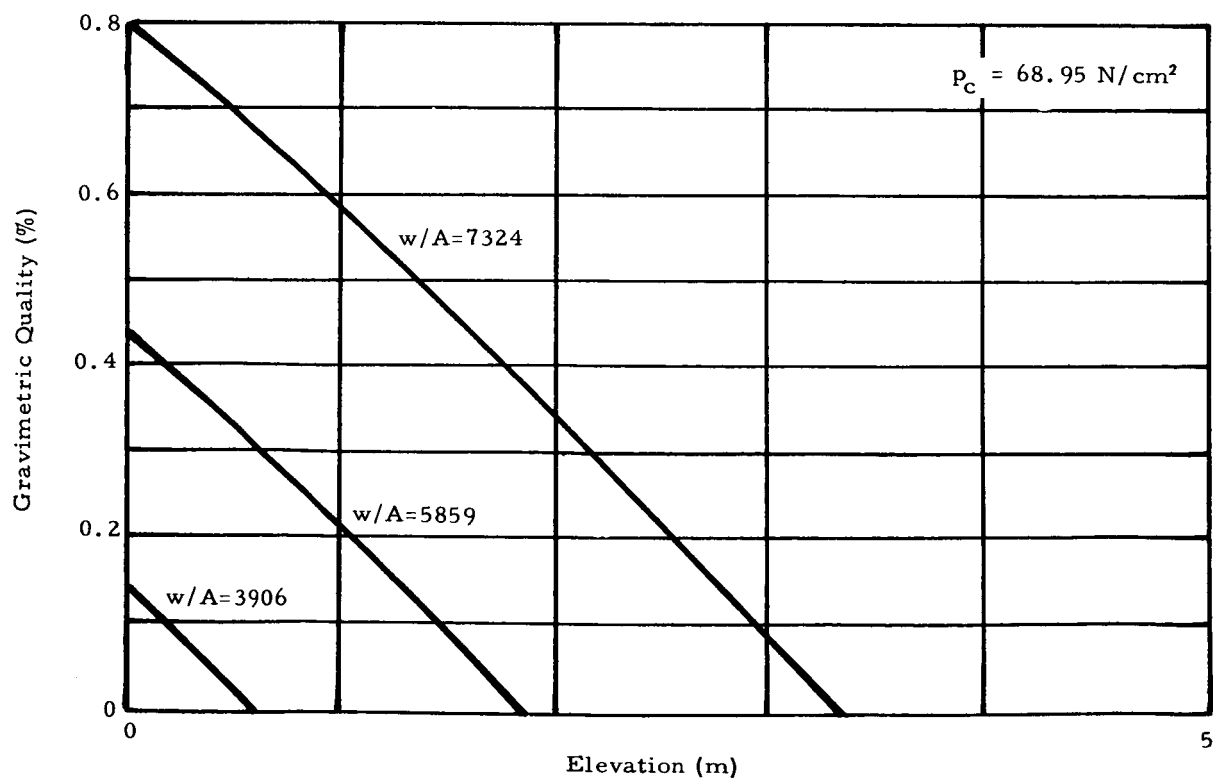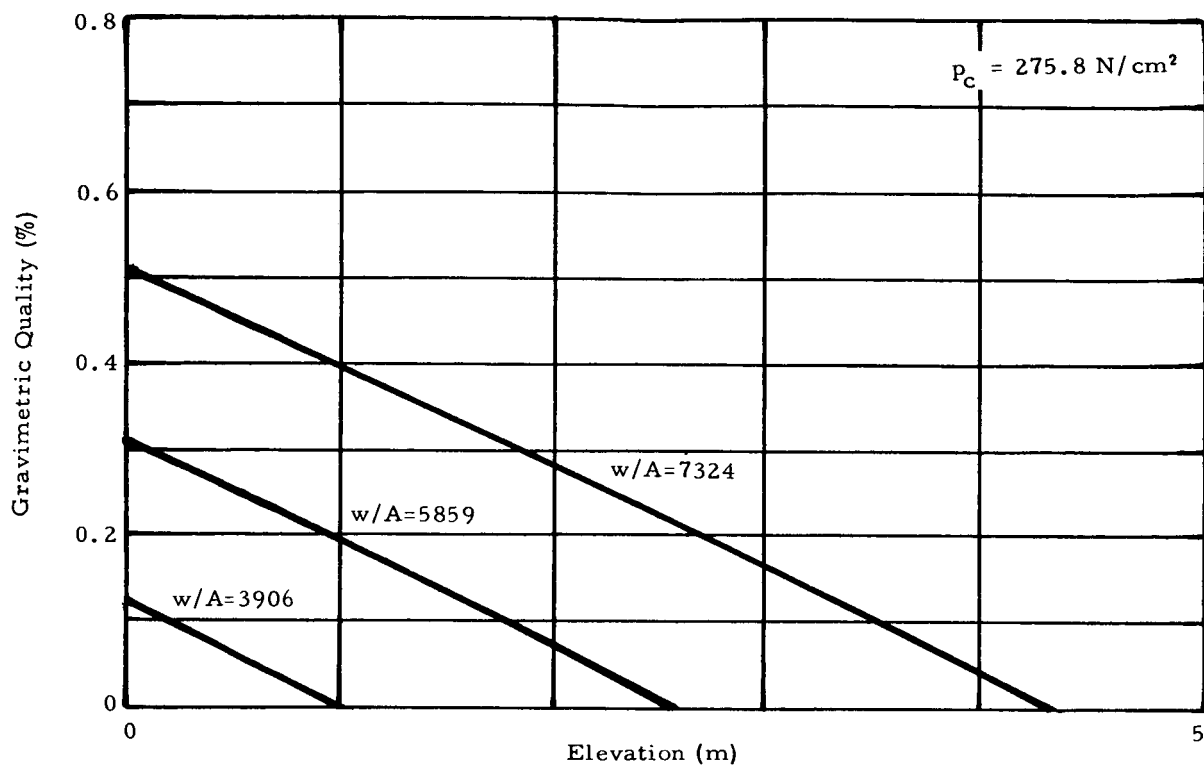
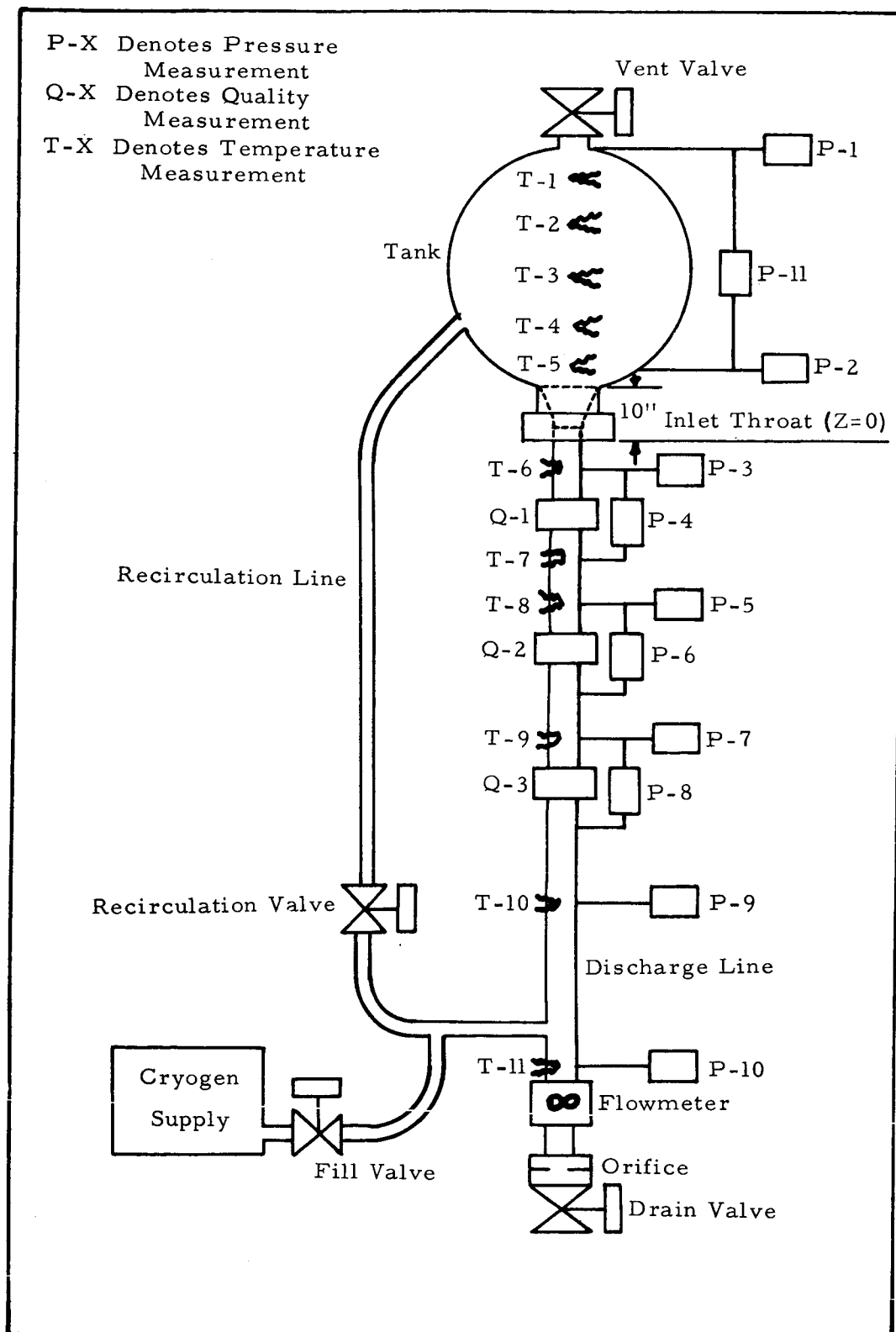FIG 18 Quality versus Elevation for Oxygen (Finite Difference Solution)
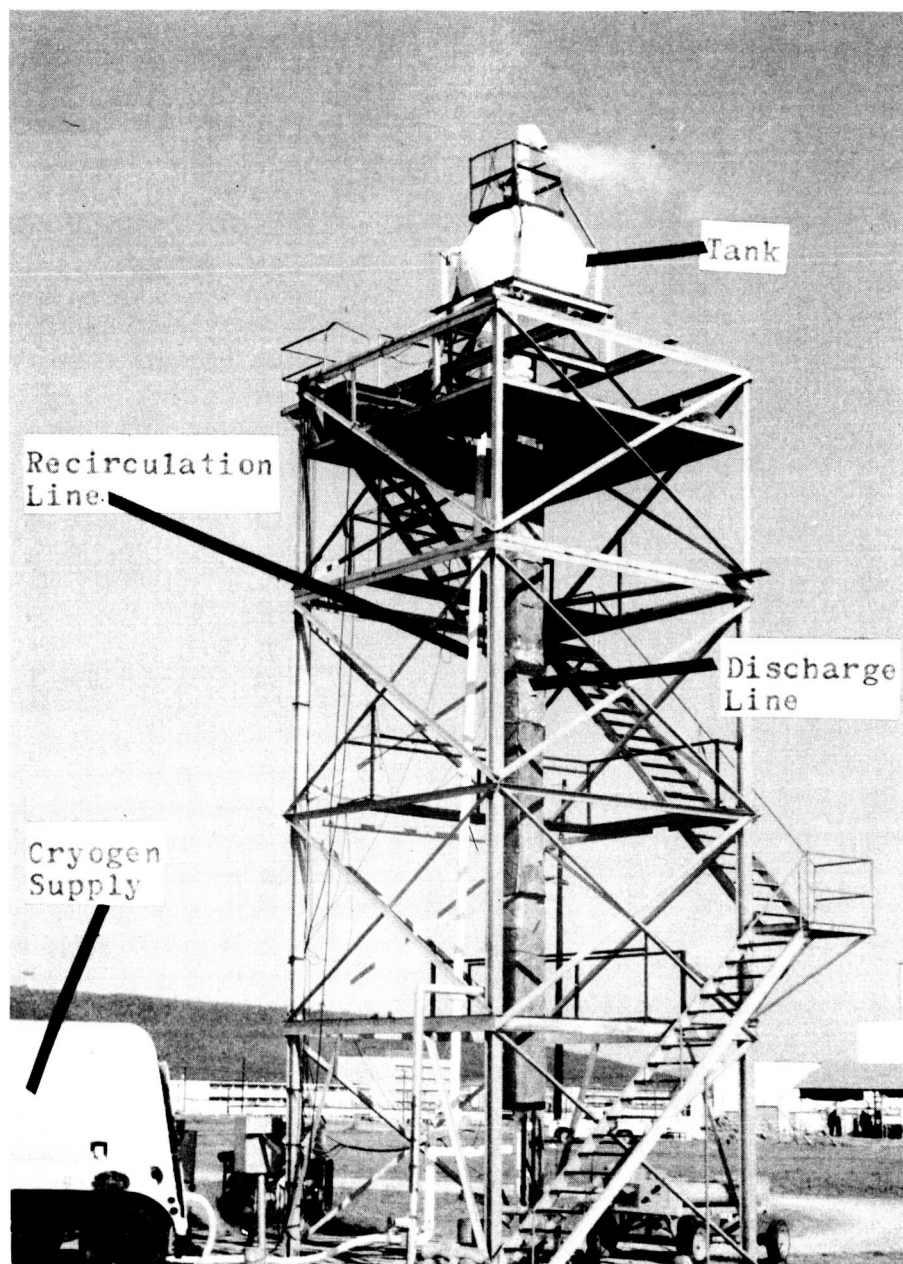
FIG 19 Experimental Apparatus Schematic

FIG 20 Experimental Apparatus

Table I Component Description

Component	Manufacturer	Discription
Tank	German Government	1.727 m inside diameter spherical aluminum tank with 2.54 cm thick shell
Discharge Line		15.24 cm diameter 6061 aluminum pipe with 0.953 cm thick wall and flanged joints
Recirculation Line		10.16 cm inside diameter stainless steel pipe with 0.635 cm thick wall and flanged joints
Vent Valve	Parker Aircraft Company	15.24 cm diameter ball valve with pneumatic operator
Drain Valve	Parker Aircraft Company	15.24 cm diameter ball valve with pneumatic operator
Fill Valve	Hydromatics Inc.	5.08 cm diameter ball valve with pneumatic operator
Recirculation Valve	Rocketdyne	10.16 cm diameter butterfly valve with pneumatic operator
Cryogen Supply	Cambridge, Inc.	16.33 M. T. liquid oxygen capacity

	Table II	Measurement Locations
Measurement Number	Measured Property	Location
F-1	Discharge Line Flowrate	In discharge line 11.66 m below inlet throat
P-1	Static Pressure	On top of tank measuring ullage pressure
P-2	Static Pressure	On tank bottom measuring container pressure
P-3	Static Pressure	On discharge line 0.076 m below inlet throat
P-4	Difference in Static Pressure	On discharge line between 0.076 and 0.908 m below throat
P-5	Static Pressure	On discharge line 2.228 m below inlet throat
P-6	Difference in Static Pressure	On discharge line between 2.228 and 3.060 m below throat
P-7	Static Pressure	On discharge line 4.383 m below inlet throat
P-8	Difference in Static Pressure	On discharge line between 4.383 and 5.212 m below throat
P-9	Static Pressure	On discharge line 7.861 m below inlet throat
P-10	Static pressure	On discharge line 10.71 m below inlet throat
P-11	Difference in Static Pressure	Between top and bottom of tank
Q-1	Fluid Quality	In discharge line 0.457 m below inlet throat
Q-2	Fluid Quality	In discharge line 2.61 m below inlet throat
Q-3	Fluid Quality	In discharge line 4.76 m below inlet throat
T-1	Temperature	In tank on vertical axis 0.762 m above tank center
T-2	Temperature	In tank on vertical axis 0.381 m above geometric center
T-3	Temperature	In tank at geometric center
T-4	Temperature	In tank on vertical axis 0.381 m below geometric center
T-5	Temperature	In tank on vertical axis 0.762 m below geometric center
T-6	Temperature	In discharge line 0.076 m below inlet throat
T-7	Temperature	In discharge line 0.908 m below inlet throat
T-8	Temperature	In discharge line 3.060 m below inlet throat
T-9	Temperature	In discharge line 5.212 m below inlet throat
T-10	Temperature	In discharge line 7.861 m below inlet throat
T-11	Temperature	In discharge line 10.711 m below inlet throat

and bottom of the container. The temperatures inside the tank were measured with triple junction copper constantan thermopiles located symmetrically along the vertical axis of the tank, a distance of 0.381 meters (15 inches) apart. The thermopiles were mounted on a stainless steel bracket suspended from the top of the tank, and the wires were led to a reference temperature junction located outside the tank through an adapting flange between the tank and vent valve. Pressure was measured at eight locations in the discharge line. Temperatures were measured along the center line of the discharge line at eight elevations, and fluid quality was measured at three discharge line elevations. The location of all discharge line measurements is shown in Table II as a vertical distance below the inlet throat. All measurements were recorded on a 36-channel oscillograph. A discussion of the measurement equipment used in recording data from this experimental apparatus follows.

Flow Measurement

The discharge line flowrate was measured with a turbine type flowmeter. The location of the flowmeter and experimental conditions were so chosen that single-phase flow would exist at the flowmeter.

Pressure Measurements

Two types of pressure transducers were used for pressure measurements; one type (used for measuring P-4, P-6, P-8 and P-11) used a twisted Bourdon tube and the other (used for all remaining pressure measurements) was a diaphram type.

Quality Measurements

The liquid vapor quality was determined by measuring the difference in dielectric constant of the liquid and vapor. The transducers were pipe test sections with an internal capacitive matrix and temperature sensor. The matrix measured the capacitance of the fluid passing through the pipe test section. This fluid capacitance was then fed into an analog computer where it was compared to the capacitance of the liquid and vapor. The capacitance of the liquid and vapor were generated as a function of temperature using the output of the temperature sensor in the pipe test section. The volumetric liquid vapor quality appeared as a direct current output that was recorded on the oscillograph.

A block diagram of a typical quality measurement taken from reference 18 is shown in FIG 21.

Temperature Measurements

All temperatures were measured with triple junction copper constantan thermopiles. Liquid nitrogen at atmospheric pressure was used as the reference junction.

EXPERIMENTAL PROCEDURE

Before conducting an experiment, the measurement systems were calibrated, and the correct orifice was installed in the discharge line. The tank atop the tower was then filled from the cryogen storage supply, and the system was allowed to remain at rest for 30 minutes for thermal stabilization. During fill and thermal stabilization, the recirculation valve (FIG 19) was open to allow convective circulation, and the vent valve was open to prevent pressure buildup in the tank. After termal stabilization, the tank was replenished with liquid nitrogen and the vent valve was closed. The container was then allowed to pressurize by the flow of heat from the ambient surroundings to the fluid through the tank wall and recirculation line. The thermopile in the bottom of the tank (T-5, FIG 19) was monitered to insure that the liquid temperature was near saturation. When the desired container pressure was reached, the liquid was assumed to be near saturation temperature; the recirculation valve was closed, recording equipment was started, and the drain valve was opened. When the liquid was depleted, the drain valve was closed; the recirculation and vent valves were opened; recording equipment was stopped; and the residual liquid was drained into the cryogen storage supply. The vent valve was open until the apparatus returned to approximately ambient temperature, then was closed.

COMPARISON OF EXPERIMENTAL AND ANALYTICAL RESULTS

EXPERIMENTAL CONDITIONS AND RESULTS

Three experiments were conducted to verify the analysis. Experimental parameters were selected so that a range of container pressures and discharge line flowrates were considered. The experimental conditions are shown in Table III, and results are shown in FIGS 22 through
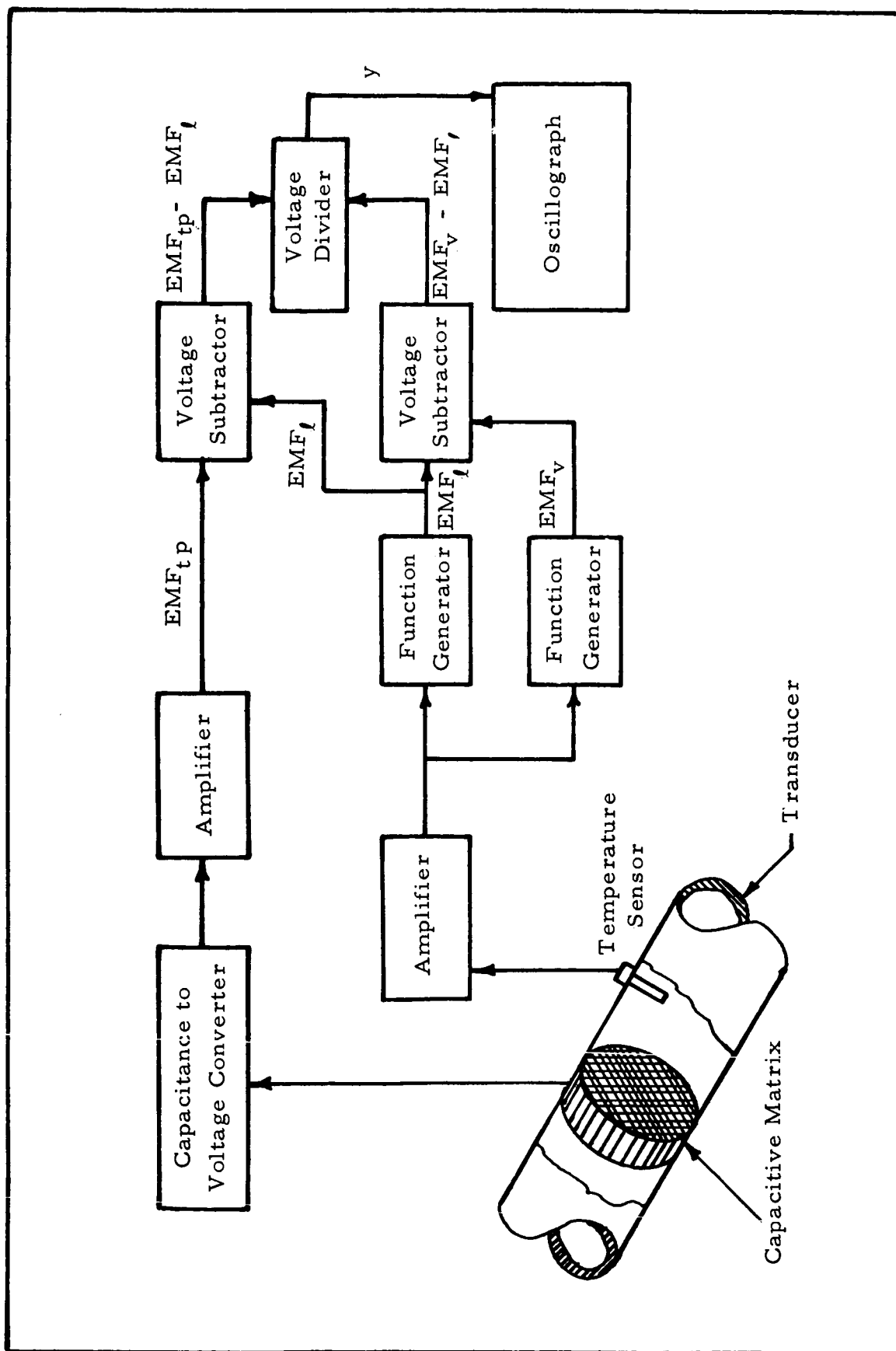
FIG 21 Typical Quality Measurement Diagram

35. The only results presented are for that portion of the discharge

TABLE III EXPERIMENTAL CONDITIONS				
Experiment Number	Orifice Diameter (cm)	Initial Container Pressure (n/cm)	Barometric Pressure (mm Hg)	Fluid
303001	7.567	51.6	745.5	Nitrogen
303002	8.158	36.3	760.5	Nitrogen
303003	8.158	64.7	768.6	Nitrogen

line in which two-phase flow exists. Conditions in the portion of the discharge line in which single-phase flow exists can be accurately determined using Bernoulli's equation, assuming constant velocity and the Darcy-Weisbach relationship for frictional pressure loss in a single-phase fluid.

DATA REDUCTION

After reducing data from an experiment, the discharge line flow-rate was converted to a weight flowrate per unit cross sectional area using the equation

$$(w/A) = 737.7\ Q \tag{74}$$

The value given by equation 74 and the container pressure P-2 (FIG 19) were then used in equations 49, 52, 71 and 73 to determine the fluid conditions in the discharge line. Pressure from the solution of equations 49, 52, 71 and 73 at an elevation of 0.076 meters (3 inches) was plotted versus time. This is shown as the dashed line in FIG 22, 27, and 32. The measured pressure at the same discharge line elevation, P-3 (FIG 19), was then plotted and is shown as the circles in the same figures. The difference in static pressure between the discharge line elevations, 0.076 meters (3 inches) and 0.908 meters (35.75 inches), was determined from the solution of equations 49, 52, 71 and 73 and plotted versus time in FIG 25, 30 and 35. The measured
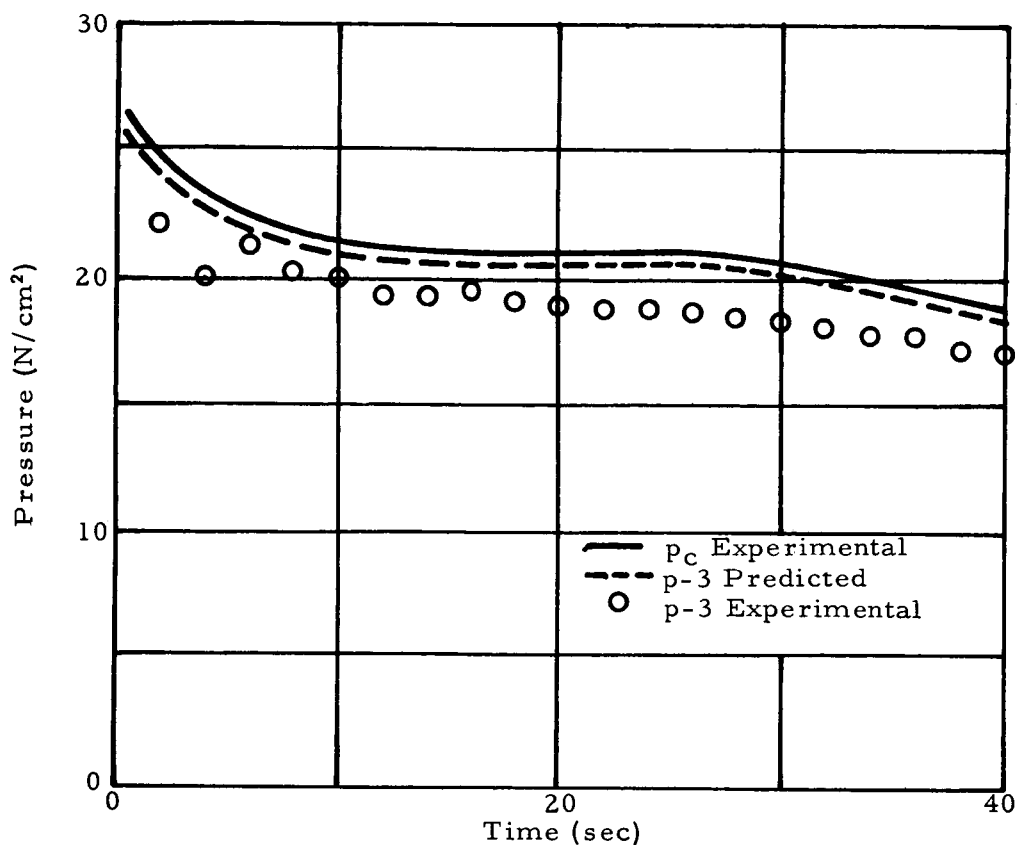
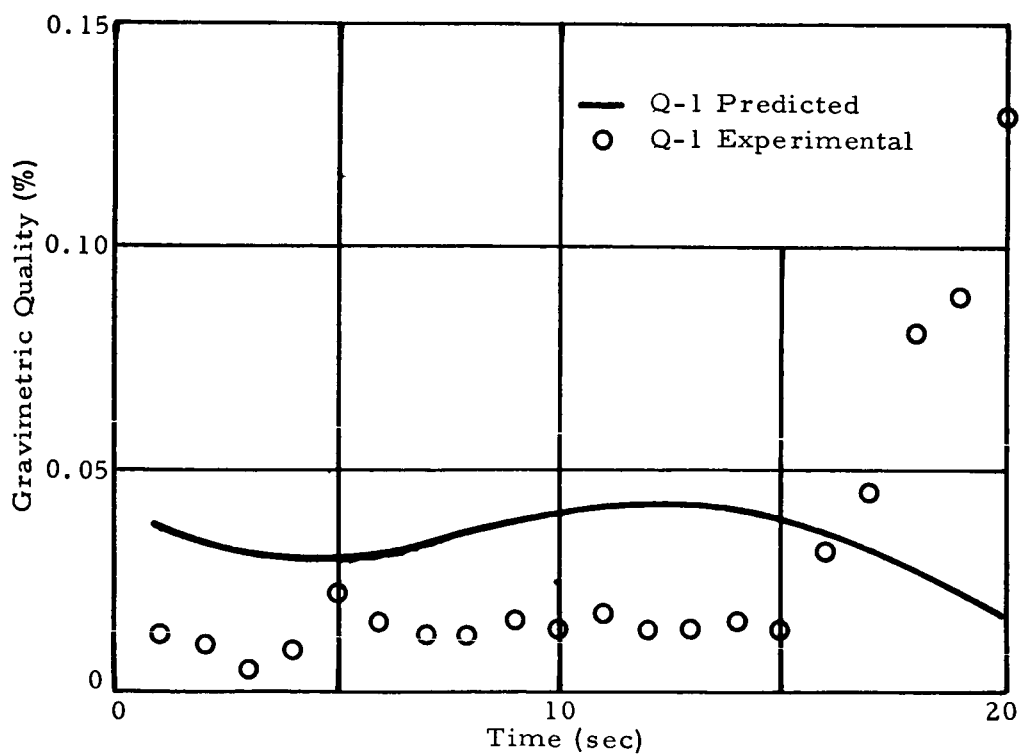FIG 22 Pressure versus Time, Experiment No. 303001

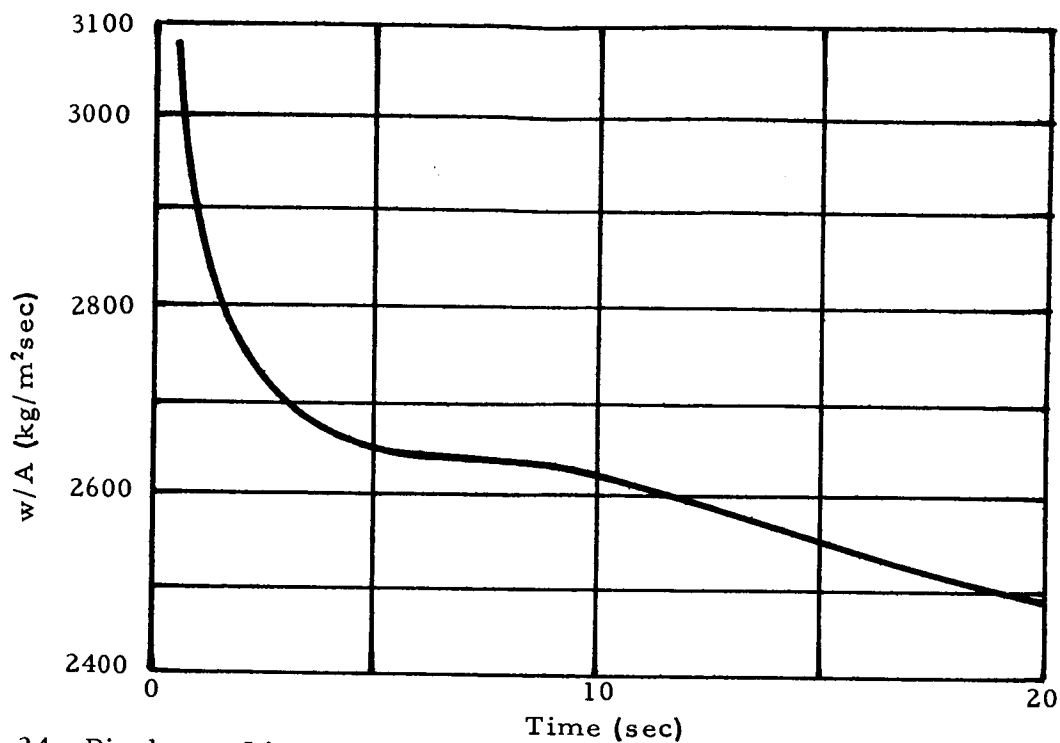FIG 23 Quality versus Time, Experiment No. 303001

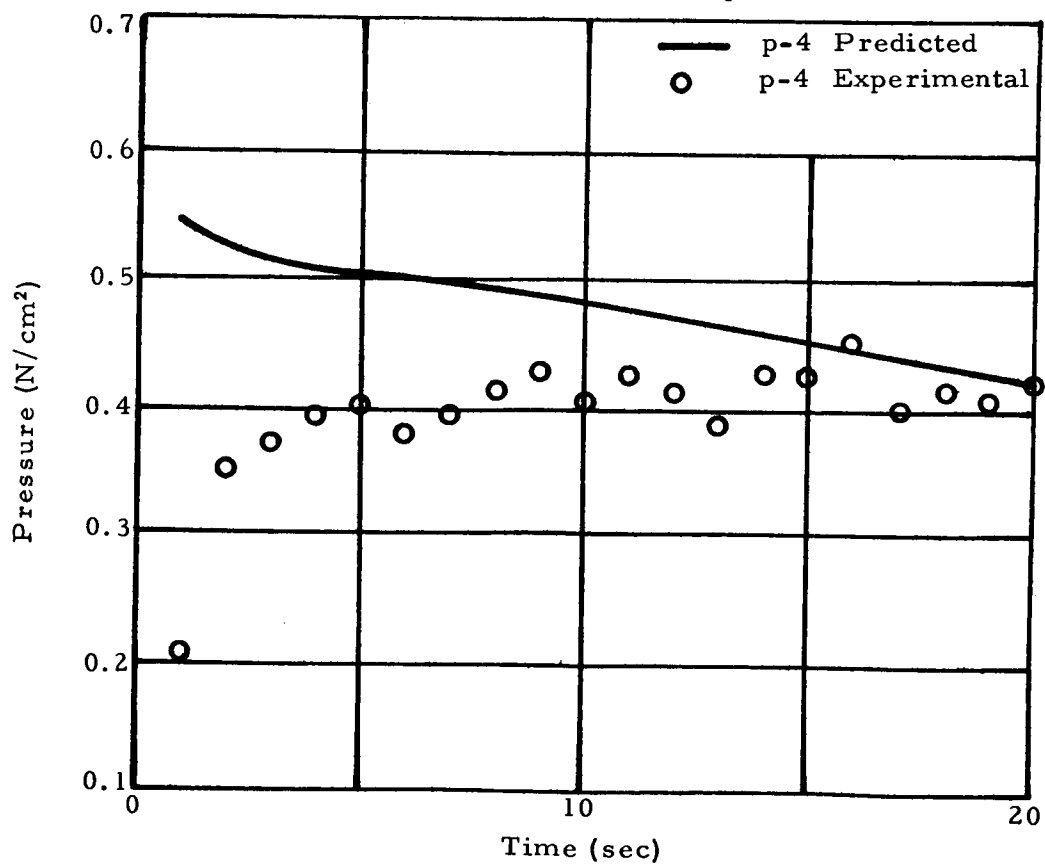FIG 24 Discharge Line Flowrate versus Time, Experiment No. 303001

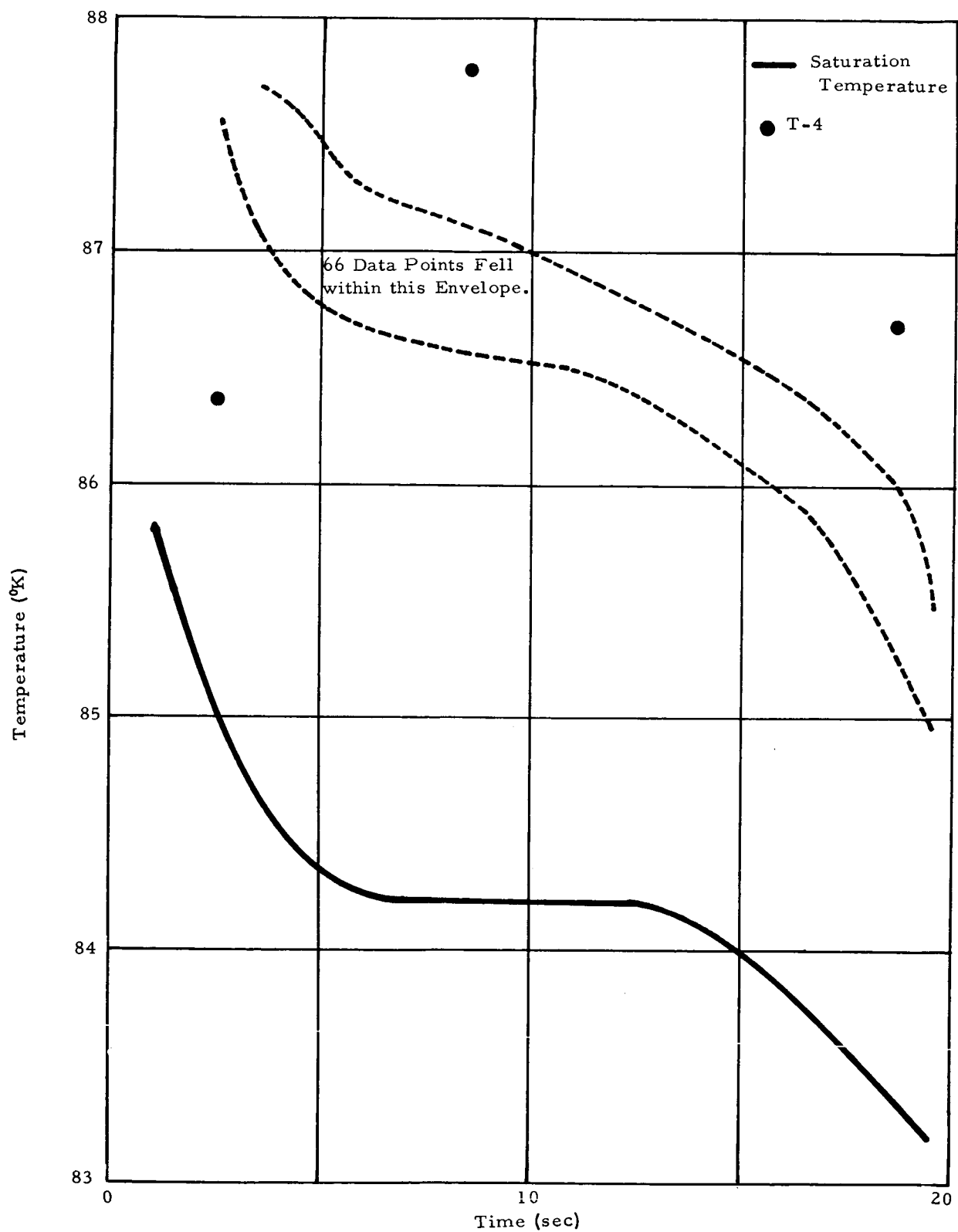FIG 25 Differential Pressure (p-4) versus Time, Experiment No. 303001

46

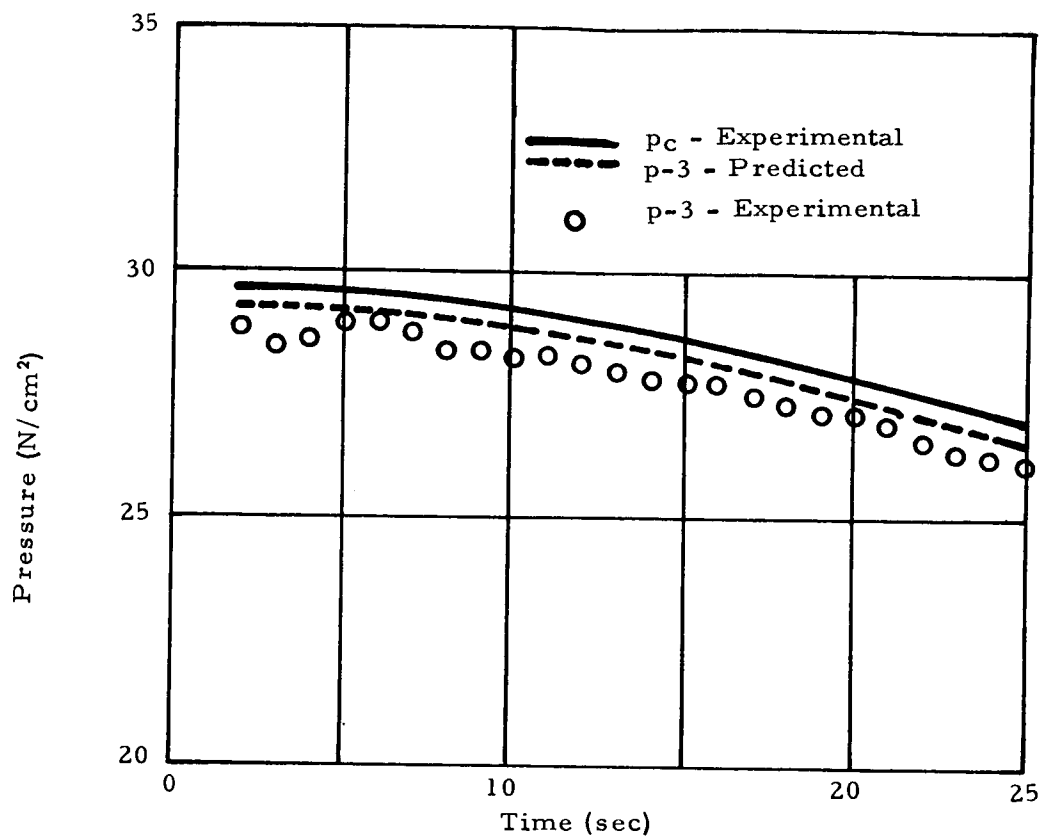FIG 26 Container Temperature versus Time, Experiment No. 303001

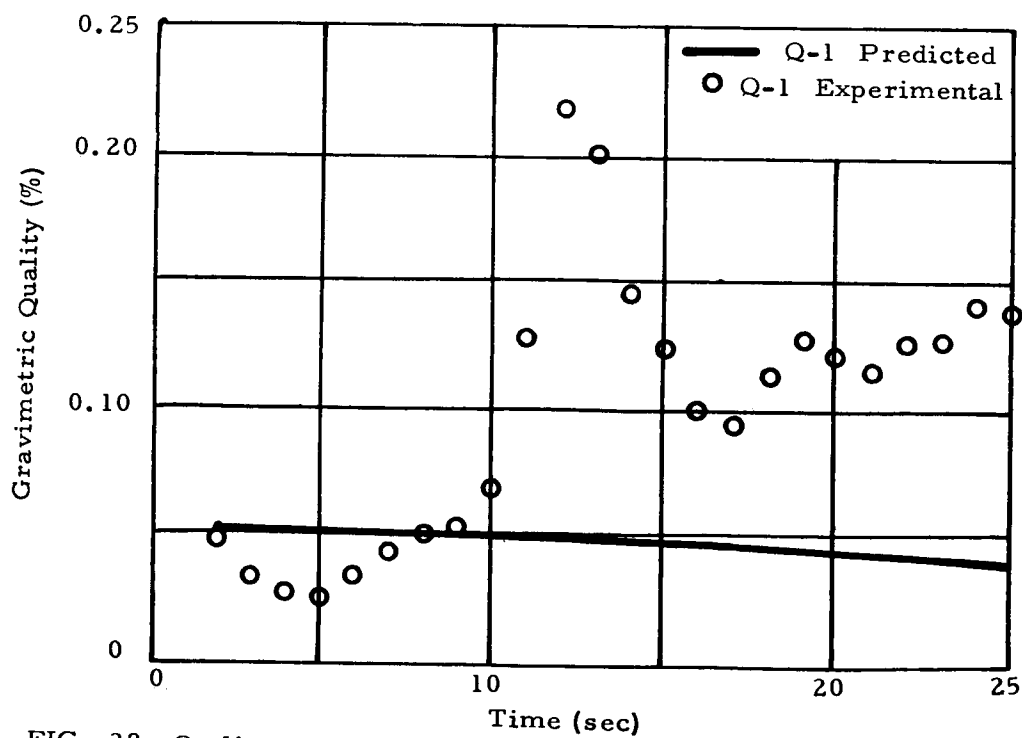FIG 27 Pressure versus Time, Experiment No. 303002

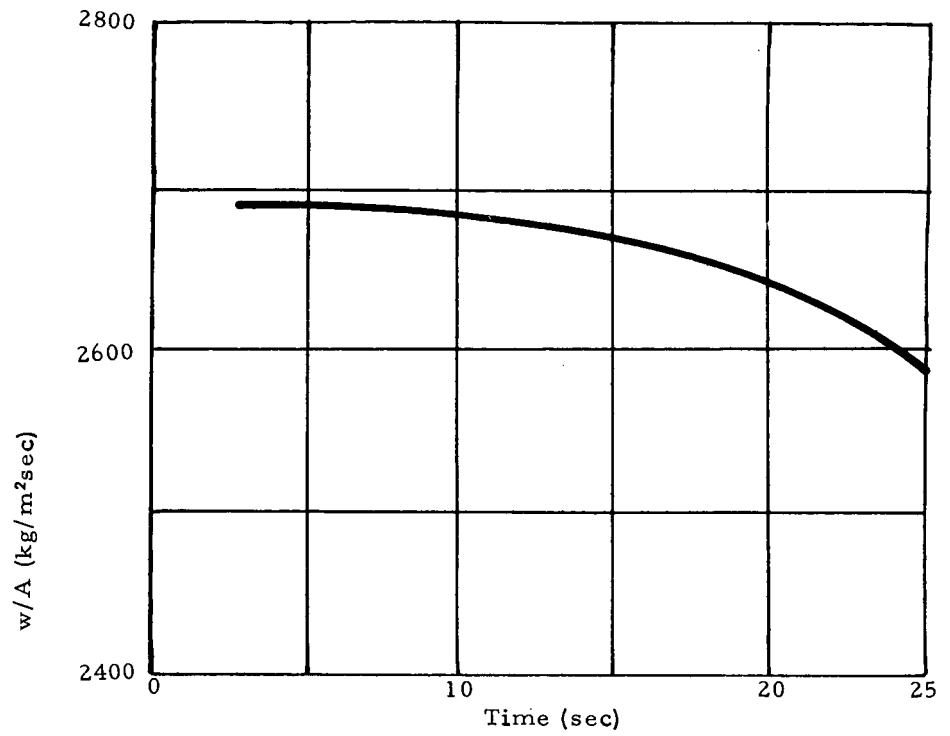FIG 28 Quality versus Time, Experiment No. 303002

FIG 29 Discharge Line Flowrate versus Time, Experiment No. 303002
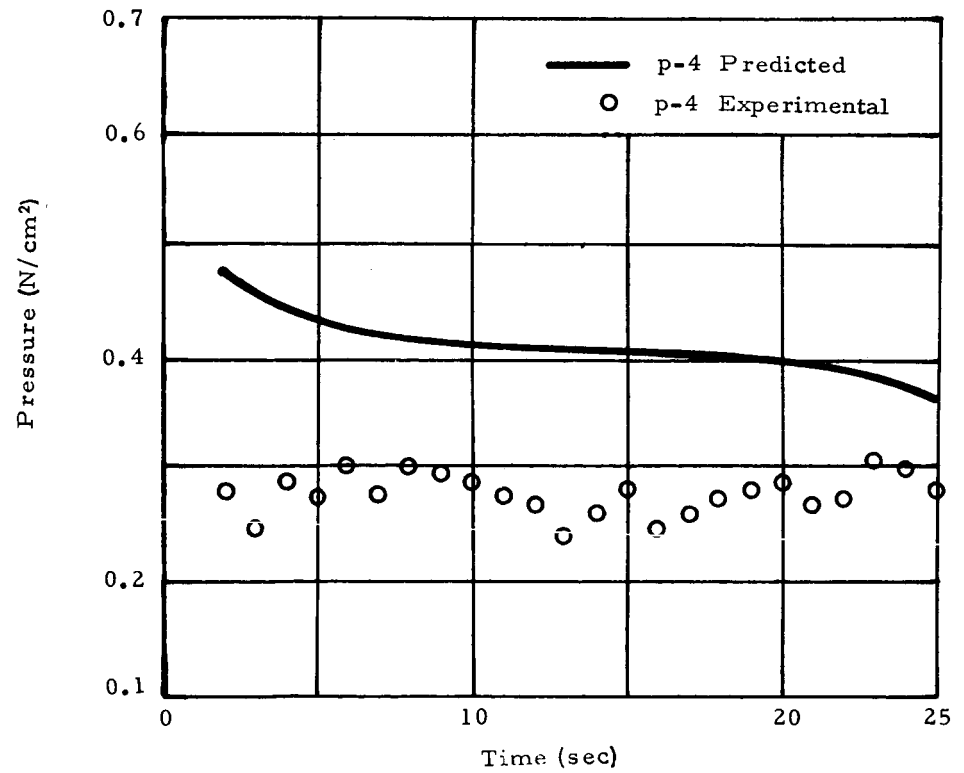

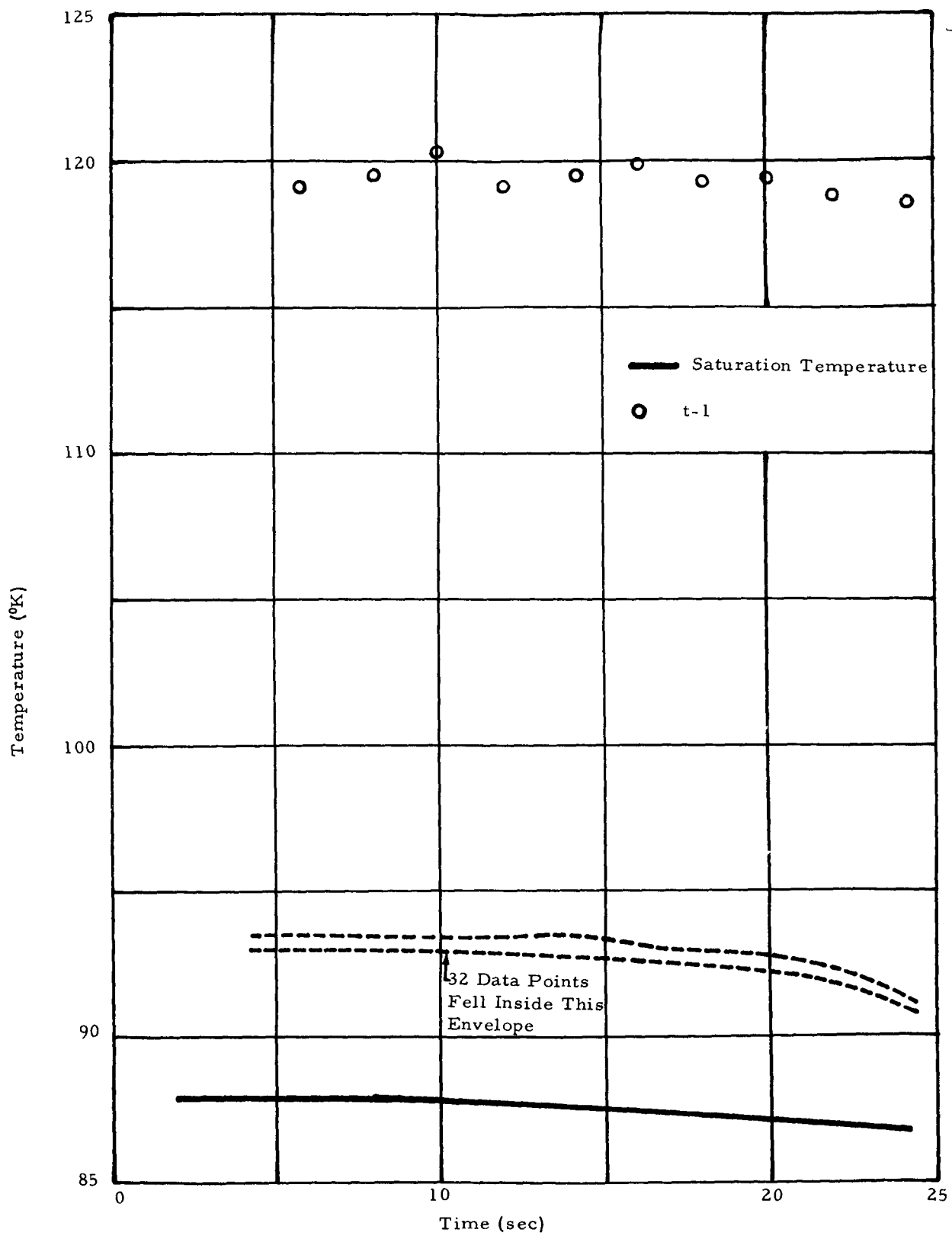FIG 30 Differential Pressure (p-4) versus Time, Experiment No. 303002

FIG   31   Container Temperature versus Time, Experiment No. 303002
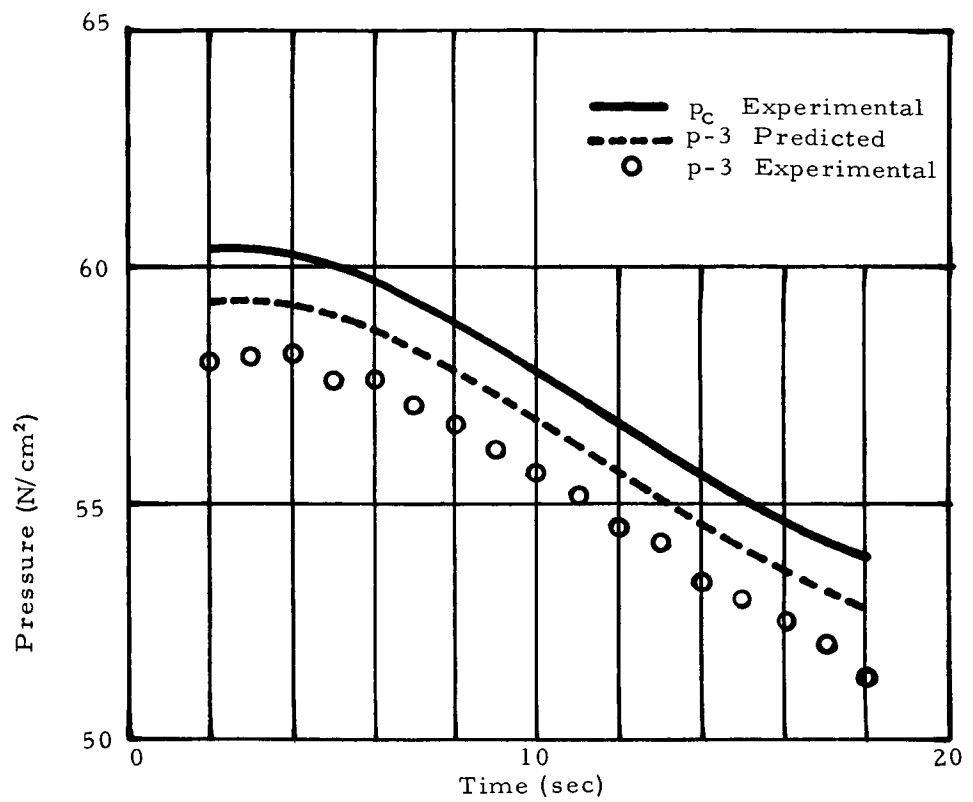
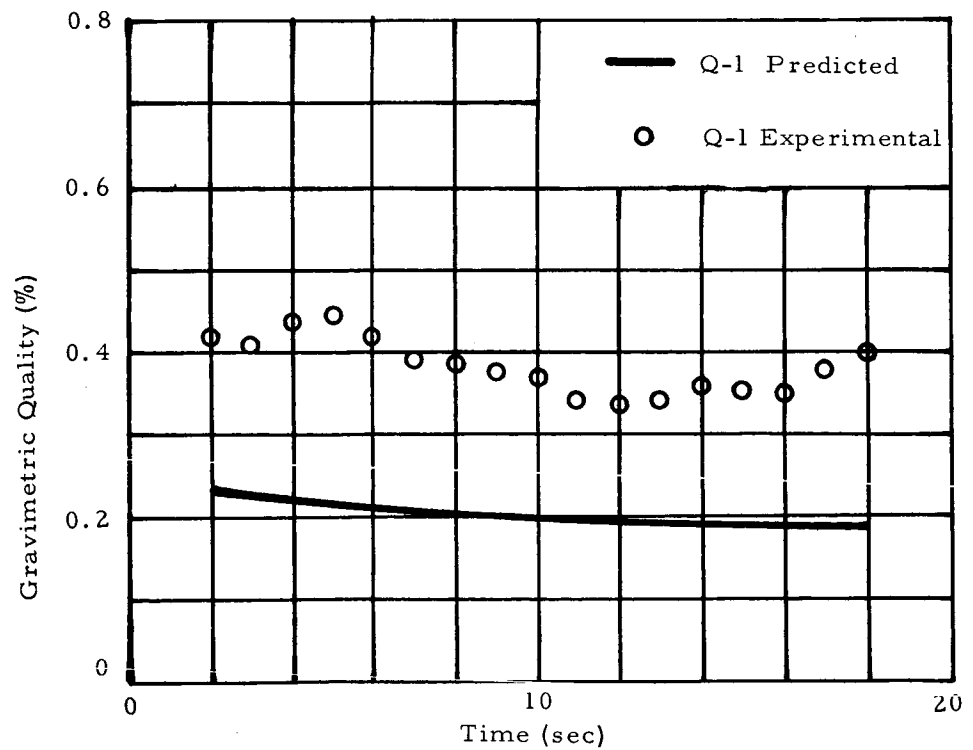FIG 32 Pressure versus Time, Experiment No. 303003

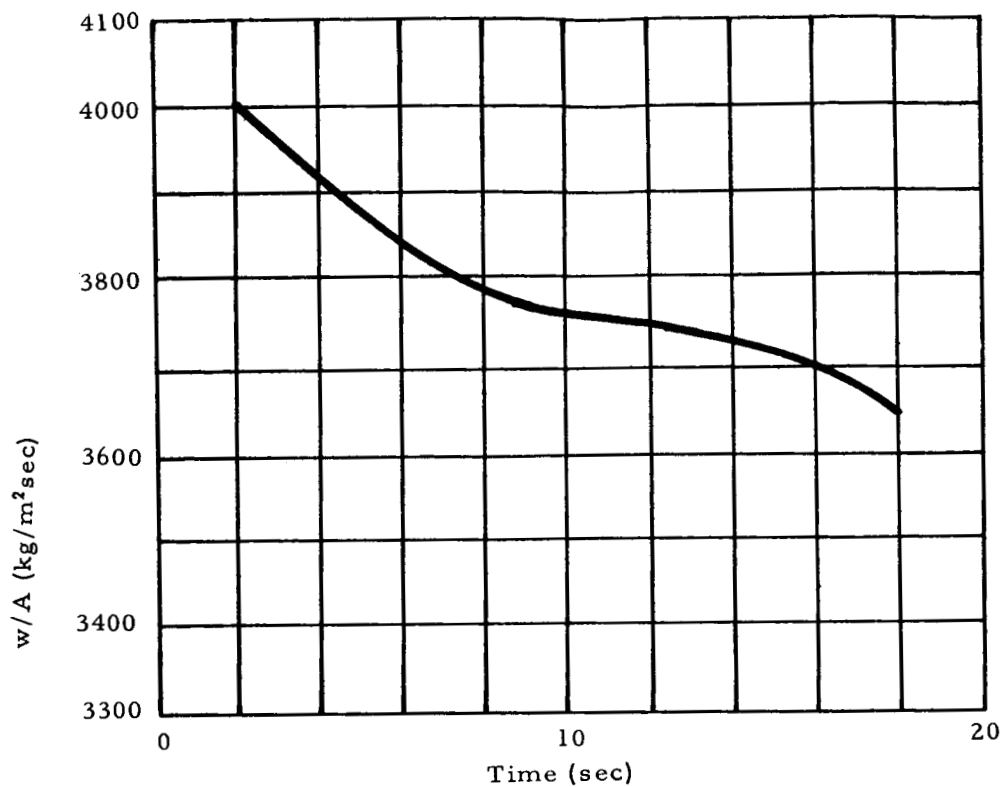FIG 33 Quality versus Time, Experiment No. 303003

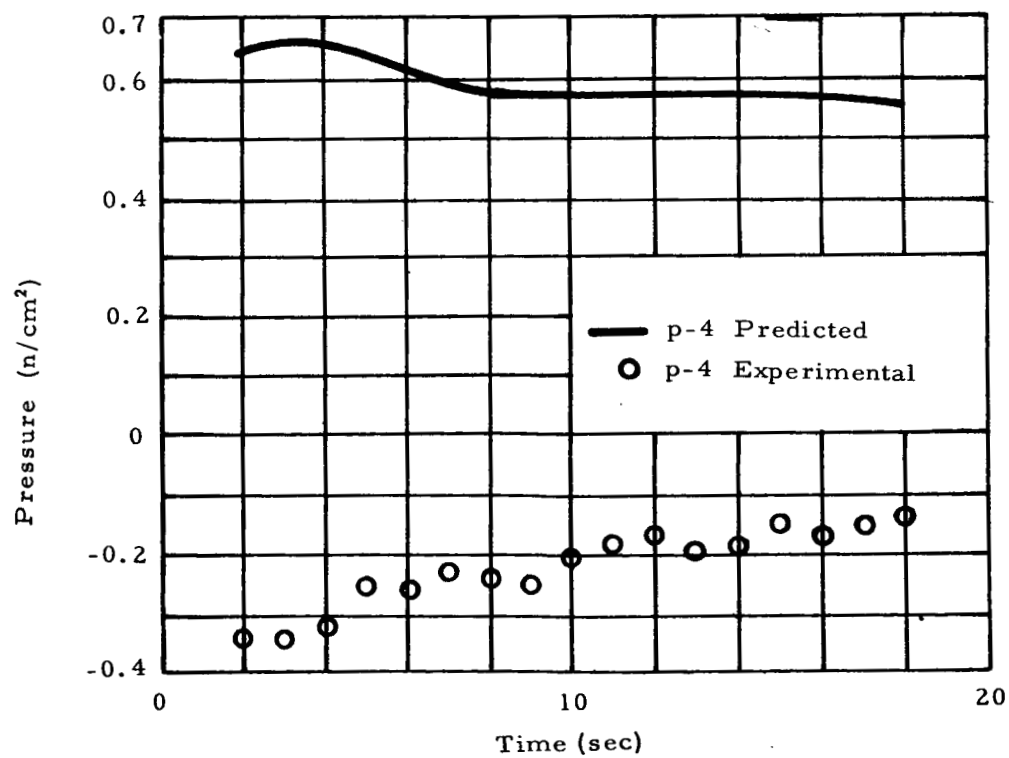FIG   34   Discharge Line Flowrate versus Time, Experiment No. 303003

FIG 35   Differential Pressure (p-4) versus Time, Experiment No. 303003

52

values of P-4 (FIG 19) were then plotted for comparison of the measured and predicted pressure difference across the capacitive matrix. No provisions were made for predicting the pressure loss caused by the capacitive matrix.

Volumetric quality from the quality measurement system was converted to a gravimetric quality using the equation

$$x = \frac{(y/v_g)}{\left[(1 - y)/v_\ell\right] + (y/v_g)} \tag{75}$$

Equation 75 is derived using a dimensional approach in reference 19. Gravimetric quality obtained from the solution of equations 49, 52, 71 and 73 at a discharge line elevation of 0.457 meters (18 inches) is plotted and compared with those measured at Q-1 (FIG 19) in FIG 23, 28 and 33.

The discharge line weight flowrate per unit cross sectional area is plotted versus time in FIG 24, 29 and 34.

For additional information on self-pressurized containers, the temperatures inside the container are plotted for two of the three experiments in FIG 26 and 31.

CONCLUSIONS

From comparison of the predicted and experimental results, it is concluded that the analytical equations will predict the fluid conditions in the discharge line when draining a self-pressurized container.

The quality measurements show that a slight amount of vapor was discharged into the discharge line during experiment No. 303001 between 30 and 40 seconds and during experiment No. 303002 between 10 and 15 seconds. A subcooled liquid was drained for the first ten seconds of experiments No. 303001 and 303002. This is evidenced by experimental qualities being less than predicted and by the large negative slope of the container pressure curve during this interval. The frictional pressure drop across the capacitive matrix was expected to be large enough to cause slightly higher than predicted qualities. These expectations were proven true by the experimental qualities and by the difference between the predicted and measured pressure differ-ence across the quality measurement matrix. This excessive frictional

53

pressure loss greatly amplified the effect of the vapor discharge into the discharge line during experiment No. 303001 and 303002. The frictional pressure drop across the capacitive matrix during experiment No. 303003 was so great that the pressure below the matrix (FIG 35) was less than the pressure above the matrix. The measured and predicted discharge line static pressure (FIG 22, 27 and 32) agreed within the limits of accuracy of the measurement system. The container temperatures did not differ significantly from the saturation temperature. The experimental phase of this program proved the analysis accurate for the case considered, but points out that any obstruction in the discharge line will cause a significant deviation from the predicted fluid conditions. To obtain extreme accuracy, the effects of obstructions must be considered. The assumption of no vapor being discharged into the discharge line was valid in almost all instances. When vapor was expelled into the discharge line, the amount was small and was neglected with a slight loss of accuracy.

This analytical technique is applicable to many other problems involving two-phase fluid flow, if the quality can be predicted at the inlet throat. An example of a problem solvable by this technique is a liquid discharge line carrying a two-phase mixture because of a vortex in the reservoir above the discharge line. In this instance the inlet quality can be predicted knowing the liquid drain rate and estimating the vapor drain rate from the size of the vortex.

REFERENCES

1. Canty, J. M., "Pressure Phenomena During Transfer of Saturated Cryogenic Fluids," Advances in Cryogenic Engineering, Vol 6, p 272, Plenum Press, New York, N. Y. 1961

2. Leonhard, K. E. and McMordie, R. K., "The Non-Adiabatic Flow of an Evaporating Cryogenic Fluid Through a Horizontal Tube," Advances in Cryogenic Engineering, Vol 6, p 481, Plenum Press, New York, N. Y. 1961

3. McAdams, W. E., Woods, W. K., Heroman, L. C., Jr., "Vaporization Inside Horizontal Tubes II-Benzene-Oil Mixtures," Transactions ASME, Vol 64, p 193, 1942

4. Benjamin, M. W. and Miller, J. G., "The Flow of a Flashing Mixture of Water and Steam Through Pipes," Transactions ASME, Vol 64, p 657, 1942

5. Davidson, W. F., Hardie, P. H., Humphries, C. G. R., Markson, A.A., Mumford A. R. and Ravese, T., "Studies of Heat Transmission Through Boiler Tubing at Pressure From 500 to 3000 Pounds," Transactions ASME, Vol 65, p 553, 1943

6. Martinelli, R. C., Boelter, L. M. K., Taylor, T. H. M., Thomsen, E. G. and Morrin, E. H., "Isothermal Pressure Drop for Two-Phase Two-Component Flow in a Horizontal Pipe," Transactions ASME, Vol 66, No 2, p 139, 1944

7. Martinelli, R. C., Putnam, J. A., and Lockhart, R. W., "Two-Phase, Two-Component Flow in the Viscous Region," Transactions AIChE, Vol 42, No 4, p 681, 1946

8. Martinelli, R. C. and Nelson, D. B., "Prediction of Pressure Drop During Forced-Circulation Boiling of Water," Transactions ASME, Vol 70, No. 8, p 695, 1948

9. Lockhart, R. W. and Martinelli, R. C., "Proposed Correlation of Data for Isothermal Two-Phase, Two-Component Flow in Pipes," Chemical Engineering Progress, Vol 45, No 1, p 39, 1949

10. Johnson, H. A. and Abou-Sabe, A. H., "Heat Transfer and Pressure Drop for Turbulent Flow of Air-Water Mixtures in a Horizontal Pipe," Transactions ASME, Vol 74, No 8, p 977, 1952

11. Harvey, B. F. and Foust, A. S., "Heat Transfer Symposium," Chemical Engineering Progress Symposium Series, Vol 49, No 5, p 91, 1953

12. Rogers, J. D., "Two-Phase Flow of Hydrogen in Horizontal Tubes," AIChE Journal, Vol 2, p 536, 1956

13. Hatch, M. R. and Jacobs, R. B., "Prediction of Pressure Drop in Two-Phase Single Component Fluid Flow," AIChE Journal, Vol 8, No 1, p 18, 1962

14. Johnson, Victor J., "A Compendium of the Properties of Materials at Low Temperature (Phase 1)," National Bureau of Standards, Cryogenic Engineering Laboratory, Contract No AF 33(616)-58-4, Wright Air Development Division Technical Report 60-S6, October 1960

15. Stewart, R. B., Hust, J. G., and McCarty, R. D., "Interim Thermodynamic Properties for Gaseous Oxygen at Temperatures From 55 to 300 K and Pressures to 300 Atmospheres," National Bureau of Standards Report No 7922, October 1963

16. Strobridge, Thomas R., "The Thermodynamic Properties of Nitrogen From 114 to 540 R Between 1.0 and 3000 psia, Supplement A (British Units)," National Bureau of Standards, Technical Note 129A, February 1963

17. Brown, Aubrey I. and Marco, Salvatorie M., "Introduction to Heat Transfer," third ed., McGraw-Hill Book Company Inc., New York, N. Y. 1963, pp 97-123

18. "Instruction Manual for the Model 206-1 Quality Measurement System," Space Sciences Inc., Document No SSI-206-MA, Waltham, Massachusetts, 1964, pp 1-7

19. Campbell, Hugh M., Jr., "Phase Change in a Low Quality Single Component Fluid Flowing Vertically Downward in a Tube," Masters Thesis, University of Alabama, 1965, pp 66-68

FLUID QUALITY IN A SELF-PRESSURIZED
CONTAINER DISCHARGE LINE

By Hugh M. Campbell, Jr.

The information in this report has been reviewed for security classification. Review of any information concerning Department of Defense or Atomic Energy Commission programs has been made by the MSFC Security Classification Officer. This report, in its entirety, has been determined to be unclassified.

This document has also been reviewed and approved for technical accuracy.

W. E. DICKSON
Chief, Propulsion Cryogenics Section

R. R. HEAD
Chief, Applied Mechanical Research Branch

H. G. PAUL
Chief, Propulsion Division

F. B. CLINE
Director, Propulsion and Vehicle Engineering Laboratory

BIBLIOGRAPHY

Binder, R. C., "Fluid Mechanics," third ed., Prentice-Hall Inc., Englewood Gliffs, N. J., 1956

Hawkins, George A., "Thermodynamics," John Wiley and Sons Inc., New York, N. Y., 1962

Scott, R. B., "Cryogenic Engineering," D. Van Nostrand Company, New York, N. Y., 1959

Shapiro, Ascher H., "The Dynamics and Thermodynamics of Compressible Fluid Flow," Vol I, The Ronald Press Company, New York, N. Y., 1953

Van Wylen, Gorden J., "Themodynamics," second ed, John Wiley and Sons Inc., New York, N. Y., 1962

DISTRIBUTION

R-DIR	Mr. Weidner
R-ASTRO-DIR	Dr. Haeussermann
R-ASTRO-N	Mr. Moore
R-ME-DIR	Mr. Kuers
R-QUAL-DIR	Mr. Grau
R-RP-DIR	Dr. Stuhlinger
R-TEST-DIR	Mr. Heimburg
R-TEST-C	Mr. Halbrooks
R-TEST-T	Mr. Driscoll
R-TEST-SP	Mr. Pearson
R-P&VE-DIR	Mr. Cline
R-P&VE-M	Dr. Lucas
R-P&VE-S	Mr. Kroll
R-P&VE-V	Mr. Aberg
R-P&VE-P	Mr. Paul
R-P&VE-P	Mr. McCool
R-P&VE-PA	Mr. Thomson
R-P&VE-PE	Dr. Head (25)
R-P&VE-PM	Mr. Fuhrmann
R-P&VE-PP	Mr. Heusinger
R-P&VE-PT	Mr. Wood
R-P&VE-PT	Mr. Worlund
R-P&VE-PT	Mr. Helms
R-P&VE-PR	Mr. Eby
R-P&VE-RT	Mr. Hofues
MS-I	Mr. Remer
MS-H	Mr. Akens
K-DIR	Dr. Debus
MS-T (5)	
CC-P	
HME-P	

Scientific and Technical Information Facility   (25 copies)
Attn: NASA Representative (S-AK/RKT)
P. O. Box 33
College Park, Maryland   20740

Defense Documentation Center   (20 copies)
Cameron Station
Alexandria, Virginia   22314

IKOR
39 A Green Street
Waltham, Massachussetts